A study on the spacing between the centrosomes

中心体が距離を取り配置する機構の研究

Fujii, Ken

Doctor of Philosophy

Department of Genetics

School of Life Science

The Graduate University for Advanced Studies, SOKENDAI

Cell Architecture Laboratory

National Institute of Genetics

2022 (school year)

TABLE OF CONTENTS

ABSTRACT

The centrosome is a major microtubule-organizing center in animal cells. The position of the centrosome inside the cell is important for the cell's functions. Multiple centrosomes sharing a common cytoplasm are observed to position themselves by taking a certain distance among them. As a mechanism of this spacing between the centrosomes, a sliding of anti-parallel microtubules between the centrosomes using kinesin motor proteins has been known. The existence of an additional, kinesin-independent mechanism for the centrosome spacing has been suspected but uncharacterized. The characterization of the spacing mechanism between the centrosomes has been difficult because the cell nucleus and chromosomes are often located between the centrosomes and they hinder the investigation of the direct interaction between the centrosomes.

In this study, I addressed the mechanisms underlying the spacing activity between the centrosomes using the *Caenorhabditis elegans* embryo. Previous studies suggested that kinesins required for the known spacing mechanism in other species are not required for the spacing in the *C. elegans* embryo. To characterize the spacing mechanism in the *C. elegans* embryo, I developed a method to remove the chromosomes from the embryo to focus on the interaction between the centrosomes by excluding the effect from the cell nucleus and chromosomes. In the enucleated embryos, the space between the sister centrosomes increased after the centrosome duplication. The observation demonstrated that the enucleated *C. elegans* embryo is a good model to address the mechanisms underlying the spacing activity.

To investigate the mechanism of the spacing activity between the centrosomes, I searched for the genes required for the spacing activity in the enucleated *C. elegans* embryos. The cortical pulling force is a force generated by force generators at the cell cortex. I first knocked down *gpr-1/2 genes*, which are essential for generating the cortical pulling force. The knockdown impaired the spacing, but not completely. The result suggested that the cortical pulling force contributes to the spacing, but is not the sole driving force. Next, I knocked down *dhc-1* gene, which encodes the catalytic subunit of dynein motor protein. Without dynein, the centrosome spacing was almost completely impaired. In addition to the cortical pulling force, dynein generates "cytoplasmic pulling force", which means the force to pull the microtubule and the centrosomes at the cytoplasmic locations such as intracellular organelles. Therefore, I inhibited both pulling forces simultaneously. Simultaneous inhibition impaired spacing of centrosomes as severe as *dhc-1* (RNAi). In conclusion, the cortical and cytoplasmic pulling forces provide major driving force for the spacing activity between the centrosomes, independent of the nucleus and chromosomes.

Next, I investigated the physical mechanism for the spacing between the centrosomes. As a mechanism to enable a pair of the centrosomes moving to different directions, I proposed the "pulling force competition model". In this model, the multiple centrosomes compete for each of the force generators located in the cell cortex or cytoplasm, and the nearer centrosome has the greater chance to be pulled by the force generator. A numerical simulation reproduced the centrosome spacing in enucleated embryos. Importantly, the model reproduced the separation of the centrosome along the surface of the nucleus as well as the centration of the centrosome and associated nucleus

in the 1-cell stage *C. elegans* embryos. These results collectively support the pulling force competition accounts for the centrosome spacing.

In addition to the mechanism of the centrosome spacing, I found an interesting behavior of the centrosomes in the enucleated *C. elegans* embryo when dynein is knocked down. My observations detected massive movement of the centrosomes, not for a while after the centrosome duplication but later at the cell cycle. I knocked down a non-muscle myosin gene (*nmy-2*), which is required for cytoplasmic flow, together with *dhc-1*, the movement of the centrosomes was almost completely blocked. The result indicated that cytoplasmic flow can move the centrosomes even when the dynein function is impaired.

Finally, I also found an unexpected dynamic of the centrosomes in enucleated, dynein knocked down embryos. After the centrosomes are dispersed in the cytoplasm with the cytoplasmic flow, they assemble to come close to each other. The mechanisms underlying the novel assembly behavior are totally mysterious, and will be an interesting topic for future research.

In summary, I found a novel type of the spacing activity of the centrosome that depends on dynein. I propose the pulling force competition model for the spacing between centrosomes. In addition, I found a floating movement of the centrosome driven by the cytoplasmic flow. Finally, I found a mysterious assembly movement of the centrosome. My study characterized novel positioning behaviors and mechanisms of the centrosomes inside the cell in *C. elegans*, which should be applicable to other organisms.

INTRODUCTION

The centrosome is an organelle in animal cells, and serves as a major microtubule organizing center (MTOC) (Wu and Akhmanove, 2017). MTOC is an intracellular structure from which the microtubules that consist of α- and β-tubulin proteins elongate (Chaaban et al., 2018). The centrosomes play important roles in cells, such as intracellular transport and cell division (O'Connell, 1999; Meraldi, 2015). For example, Golgi apparatus, yolk granules and lysosomes are transported by motor proteins moving along the microtubules toward the centrosome (Rois and Bornens, 2003; Kimura and Kimura, 2011). Importantly, the number of the centrosomes is strictly regulated inside the cell (Tsou and Stearns, 2006). The centrosome duplicates once per cell cycle, and as a result, there are one or two centrosomes in a typical cell.

Because the centrosome plays a central role in defining the spatial organization of the cell, the positions of the centrosomes in the cell are important for cellular functions (Tang and Marshall, 2012; Elric and Etienne-Manneville, 2014). In the interphase, the centrosome tends to be located at the cell center (Fig. 1A (iii)). Because the centrosome is associated with the nucleus, this positioning is important to position the nucleus at the cell center, and to position the mitotic spindle at the cell center for symmetric cell division (Silkworth et al., 2011). In the mitotic phase, the two centrosomes become the poles of the mitotic spindle (Fig. 1A (v) and (ix)). The elongation of the spindle is driven by the movement of the two centrosomes to the opposite direction, which contributes to the segregation of chromosomes during mitosis. In addition, the position of the centrosomes defines the angle and the position of the mitotic spindle, which in turn defines the cell division plane (Fig. 1A (vi)). The

direction of cell division is important for proper arrangements of cells during development (Tang and Marshall, 2012). This is because proper cellular arrangements are necessary for adjacent cells to communicate with each other during animal development. For an asymmetric cell division (Fig. 1A (vi), an off-centered positioning of the spindle often plays a critical role (Grill et al., 2001). Thus, the proper positioning of the centrosome is important for cell division and development.

The position of the centrosomes is controlled by forces generated by microtubules and motor proteins associated with the microtubules. Using the microtubule and motor proteins, the centrosome interacts with various structures, such as the cell cortex, cytoplasmic vesicles, the nucleus, the chromosomes, as well as other centrosomes. When a microtubule elongating from the centrosome encounters a cell cortex, the microtubule pushes the cortex and the cortex pushes back the microtubule to move the centrosome away from the cortex ("pushing force") (Fig. 1B (i)) (Dogterom and Yurke, 1997). Minus-end directed motor proteins that pull the microtubule often localize to the cell cortex to pull the centrosomes toward the cortex ("cortical pulling force") (Fig. 1B (ii)) (Grill and Hyman, 2005). Minus-end directed motor located at cytoplasmic vesicles pulls the centrosomes throughout the cytoplasm to position the centrosome at the cell center ("cytoplasmic pulling force") (Fig. 1B (iii) (Kimura and Kimura, 2011). Minus-end directed motor also localizes on the nuclear surface, and the centrosome slides along the nuclear surface (Fig. 1B (iv)) (Gönczy et al., 1999; Malone et al., 2003). In the mitotic spindle, each of the sister chromosomes associates one of the two centrosomes (spindle poles), and the cohesion of the chromosomes tethers the two centrosomes (Mogilner et al., 2006) (Fig. 1B (v)). In addition to these intracellular structures, centrosomes interact with each other to position themselves (Fig. 1C).

The two centrosomes sharing a common cytoplasm repulse each other. Such repulsive movement is observed after the centrosome duplication (Fig. 1A (i) to (ii), (vii) to (viii), (x) to (xi)). The resultant two centrosomes depart from each other along the surface of the nucleus, which is known as the process of centrosome separation. An intensively studied example of the repulsion/spacing activity between the centrosomes is the formation and elongation of the mitotic spindle (Brust-Mascher et al., 2004). A plus-end-directed motor protein, kinesin-5, binds to anti-parallel microtubules elongating from each of the two centrosomes (Fig. 1C (i)). When kinesin-5 motors move toward the elongating tips (plus ends) of the anti-parallel microtubules, the movement slides the microtubules apart and increases the space between the two centrosomes (Tao et al., 2006; Cheerambathur et al., 2008; Reinemann et al., 2017). This spacing mechanism in mitotic spindle involving anti-parallel microtubule and kinesin motors likely function in the spacing between the centrosomes also in interphase, in addition to mitotic spindles (Baker et al., 1993). When more than a pair of the centrosome share a common cytoplasm, which may be induced artificially or occurs naturally in syncytium, the multiple centrosomes that do not contain the chromosomes in between also show a spacing (Fig. 1C (ii)). In a classic experiment demonstrating the formation of a cell division furrow between non-sister pairs of centrosomes (i.e., the "Rappaport furrow"), these pairs were observed taking space from each other (Fig. 1C (iii)) (Oegema and Mitchison, 1997). In *Drosophila* syncytium cells, the nuclei and spindles position themselves with a certain spacing, suggesting a repulsive interaction between the centrosomes (Kanesaki et al., 2011; Telley et al., 2012; de-Carvalho et al., 2022). While the molecular mechanism of the spacing has not been studied for the Rappaport furrow case, recent studies support the sliding of plus-end-directed motors

between anti-parallel microtubules as the underlying mechanism for the repulsive interaction for non-sister pairs of the centrosomes. In *Drosophila* syncytium, a homotetrameric bipolar kinesin-5 (Klp61F), a homodimeric microtubule bundling protein PRC1 (Fascetto/Foe), and kinesin-4 (Klp3A) were demonstrated to be localized on anti-parallel microtubules where between the centrosomes and slide anti-parallel microtubules required for the spacing (Deshpande et al., 2021). PRC1 (Prc1E) and kinesin-4 (Kif4A) were also shown to separate the centrosomes in *Xenopus* egg extract (Nguyen et al., 2014, 2017). A anti-parallel sliding mechanism by kinesin-5 was assumed to function also for the centrosome separation process along the nuclear surface, without solid experimental evidence (Tanenbaum and Medema, 2010). However, for the centrosome separation process, minus-end directed motor (dynein), but not the plus-end directed motor (kinesin-5), provides a major driving force. The mechanism to repulse the two centrosomes using the minus-end directed motor remained elusive (Tanenbaum and Medema, 2010). In summary, the past knowledge on the spacing activity between the centrosomes focused on plus-end directed motor sliding along anti-parallel microtubules, and other mechanisms for the spacing between the centrosomes were not known.

In this study, I aimed to reveal a novel mechanism for the spacing between the centrosomes. From the following observations in the past, I expected that the mechanism with anti-parallel microtubules pushed apart by kinesin-5 is not the sole mechanism for the spacing. The *Caenorhabditis elegans* embryo is a well-studied model system for centrosome biology and positioning. Interestingly, unlike humans, *Xenopus,* or *Drosophila*, the *C. elegans* orthologs of the proteins involved in the sliding of anti-parallel microtubules [BMK-1 (kinesin-5 ortholog), SPD-1 (PRC1 ortholog),

and KLP-19 (kinesin-4)], are not required for the elongation of the mitotic spindle in the embryo (Powers et al., 2004; Saunders et al., 2007; Lee et al., 2015). Therefore, some other spacing mechanisms should be present in the *C. elegans* embryo because the formation and elongation of the mitotic spindle take place, as well as the centrosome separation along the nuclear surface. This suggests that an uncharacterized mechanism exists for the spacing between the two centrosomes in *C. elegans* embryos. The investigation of the uncharacterized mechanism in the *C. elegans* embryo should have impact not only for *C. elegans* biology but also for other species because kinesin independent spacing is suggested in other species (Deneke et al., 2019, Donoughe et al., 2022).

It is challenging to characterize the centrosome spacing activity, which is independent of the nucleus and spindle, in the *C. elegans* embryo. The centrosomes in the wild-type *C. elegans* embryo are consistently associated with the nucleus or spindle, and the embryonic cells do not form syncytia (Fig. 1A). Inactivation of the *zyg-12* gene offers some information on the centrosome spacing, independent of the nucleus, as this gene encodes a KASH domain protein essential for the association between the centrosome and the nucleus (Malone et al., 2003). The centrosomes move independently of the nucleus in *zyg-12*-impaired cells until the centrosomes are incorporated into the mitotic spindle during the mitotic phase. Upon inactivation of *zyg-12*, the two centrosomes in the 1-cell stage embryo separate, indicating that the spacing activity independent of the nucleus exists in the embryo. Separation is impaired by knocking down genes involved in the cortical pulling force, suggesting that this force affects the spacing (De Simone et al., 2016). However, it is unclear why the two centrosomes move in different directions instead of being pulled toward the same

cortical region (Fig. 1D). Cortical flow has been proposed to contribute to this process (De Simone et al., 2016). In the model, cortical dynein that pulls one of the centrosomes moves to a direction by cortical flow, and dynein pulling the other centrosomes moves to the opposite direction. In this mode, however, the mechanism that ensures the two centrosomes always move in the opposite directions is not clear. In addition, the cortical flow does not take place in later cell-stages, and thus this mechanism, if any, cannot be a general mechanism for the centrosome spacing. Furthermore, *zyg-12* affects the interaction between the nucleus and the centrosome, but not the spindle formation. Therefore, a spacing mechanism independent of the spindle cannot be addressed in *zyg-12*-impaired cells.

To characterize the spacing activity between the two centrosomes that is independent of the nucleus and spindle, I decided to utilize an experimental setup to remove the chromosomes from the *C. elegans* embryo ("enucleated embryo") which had been developed in my laboratory (Kimura A et al., unpublished). I expected that, using the enucleated embryo, I can reveal the positioning mechanism of the centrosomes independent of the nucleus and spindle. To create the enucleated embryo, the paternal chromosomes and the maternal chromosomes were removed using an *emb-27* mutant sperm (Sadler and Shakes, 2000) and by knockdown of the *klp-18* gene (Segbert et al., 2003), respectively. *emb-27* encodes a subunit of the anaphase-promoting complex, and its mutant causes chromosome segregation defects that produce enucleated sperm (Sadler and Shakes, 2000; Kondo and Kimura, 2019), while *klp-18* is a member of the kinesin family required for oocyte meiosis. The *klp-18* knockdown oocyte occasionally extrudes all chromosomes into the polar body and produces embryos without maternal chromosomes. By fertilizing these enucleated

sperm and oocytes, enucleated embryos are expected to be produced. In this study, I established a protocol to produce enucleated embryo in a reproducible manner, and characterized the spacing activity between the two centrosomes independent of the nucleus and spindle.

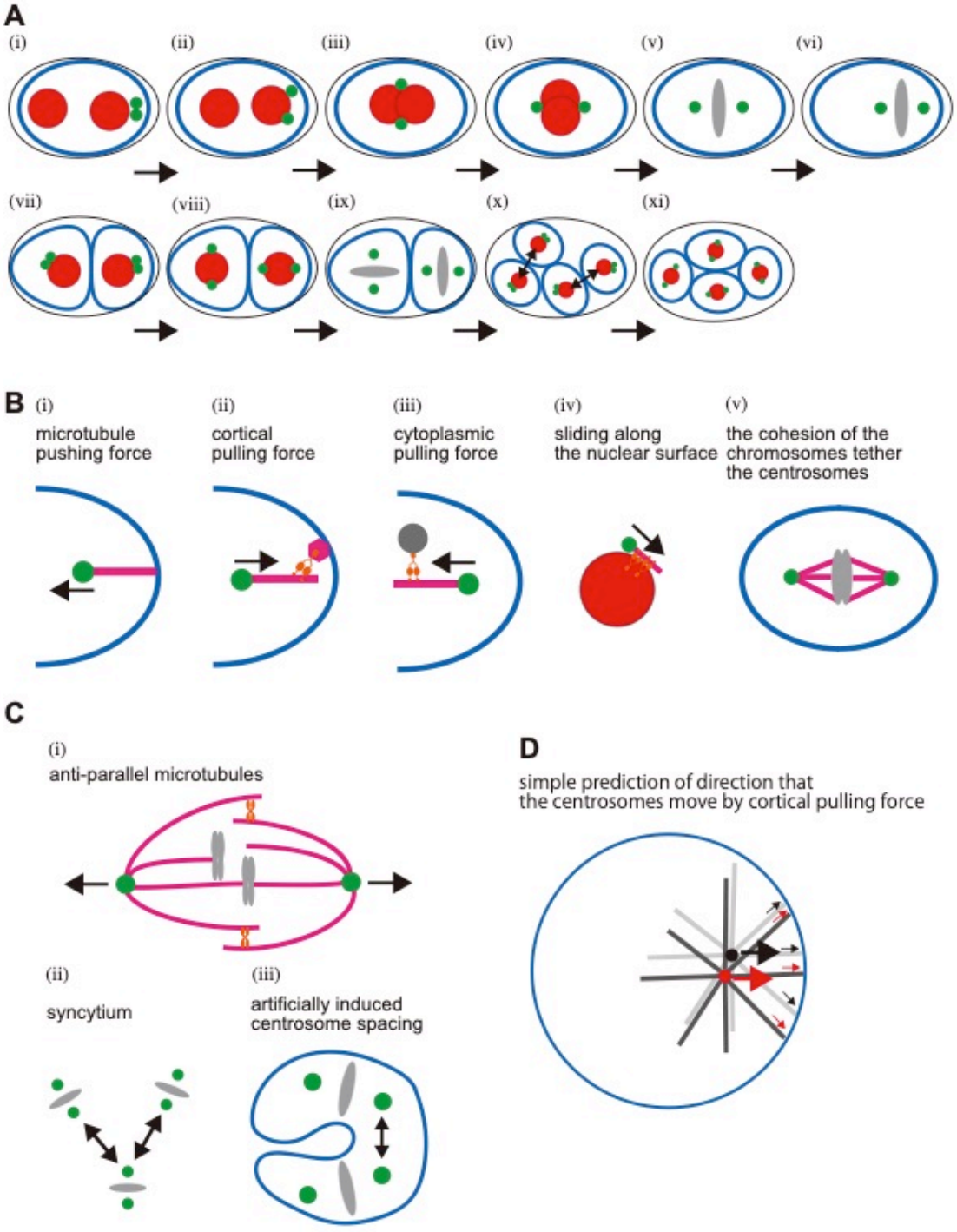

Figure 1: Drawing of the position of the centrosome and the working forces

(A) Schematic drawing of the centrosome positioning in the early embryo of *C. elegans*. The green circles indicate centrosomes, the red circles indicate nuclei, the gray ovals indicate chromosomes, and the blue ovals indicate cell membranes (in this figure). The

black ovals indicate eggshells. The 1st centrosome duplication takes place after fertilization (i). The centrosomes separate (ii), and move toward the cell center (iii). Meanwhile, the centrosome axis rotates to align along the long axis of the cell (iv). After nuclear envelope breakdown, the mitotic spindle is formed (v). The mitotic spindle of the 1-cell stage *C. elegans* embryo relocates to an off-center position (vi), which will induce an asymmetric cell division (vii). A similar dynamic positioning takes place at later cell cycles (vii ~ ix). The positions of the centrosomes define the cell division axes (x), which is important for subsequent cell arrangement (xi). (B) The forces that act to move the centrosomes. (i) The force pushing the centrosome by the extending microtubules. (ii) The force that pulls the centrosome from the cell cortex. (iii) The force of microtubules pulling intracellular organelles to move the centrosome. (iv) The centrosome sliding along the nucleus surface by the minus-end-directed motor. (v) The cohesion of the chromosomes tethers the two centrosomes. The magenta lines indicate microtubules, the orange indicates dynein, the magenta hexagon indicates cortical pulling force anchoring complex, and the gray circle indicates cytoplasmic organelle. The arrows indicate the direction in which the centrosome moves. See text for details of each force. (C) Example of the centrosome spacing. (i) The centrosomes spacing by spindle formation. (ii) The centrosome spacing in syncytium (e.g. flies). (iii) The centrosome spacing in a cell by artificial manipulation. The orange indicates kinesin-5. The arrows indicate the direction of movement of the centrosome, and the double arrows indicate the centrosome spacing. (D) When two centrosomes are located at nearby locations (e.g. just after duplication), the centrosomes should receive similar forces and move to similar directions unless there is any influence from the other centrosomes. This is unlikely the case in real cells, as we observe the spacings between the centrosomes as in (C). The red and black circles indicate

duplicated centrosomes, the black and grey lines indicate radially extending microtubules, the small red and black arrows indicate force by the cortical pulling force, and the large arrows indicate the direction in which the centrosome moves.

RESULTS

Establishment of enucleated *C. elegans* embryos by genetic manipulation

In this study, I used *C. elegans* strains in which the centrosomes (γ-tubulin), chromosomes (H2B), and cell membranes (PH) were visualized using GFP (Fig. 2, Table. 1). In control 1-cell-stage embryos, sperm- and oocyte-derived pronuclei appeared after fertilization (Fig. 2A). In the wild type, two centrosomes exist in one cell. Two centrosomes associated with the sperm pronucleus moved toward the center of the cell and met the oocyte pronucleus before the first cytokinesis (Fig. 2A, Supplemental Movie S1, Schematic drawing in Fig. 1A).

emb-27 (*g48ts*) mutant males produced enucleated sperm (Sadler and Shakes, 2000). *emb-27* mutants affect the number of centrosomes supplied by sperm (Kondo and Kimura, 2019). As a result, the presence of 1-4 centrosomes is observed in the 1-cell stage *emb-27* mutant and in the enucleated embryo. When the males were mated with the control hermaphrodite, the sperm pronucleus was absent, while the three centrosomes migrated toward the cell center to meet with the oocyte pronucleus (Fig. 2B, Supplemental Movie S2).

klp-18 (RNAi) hermaphrodites failed to undergo oocyte meiosis, and all maternal chromosomes were occasionally extruded to the polar bodies (Segbert et al., 2003). The oocyte pronucleus was not detected in these embryos during pronuclear migration (Fig. 2C, Supplemental Movie S3).

I designed an experiment to obtain embryos without chromosomes by mating *emb-27* (*g48ts*) males with *klp-18* (RNAi) hermaphrodites. In the beginning, the efficiency of obtaining enucleated embryos was low. After trials and errors, I found the

following tips to be important to improve the efficiency. Firstly, to improve the efficiency of the mating, I now mix ~25 hermaphrodites and ~125 males in a culture plate. At the beginning, I was mixing 12 hermaphrodites and 24 males to find most hermaphrodites unfertilized. By mixing 12 hermaphrodites and 60 males, the ratio of obtaining mated hermaphrodites increased to 50%. The current condition further increased the ratio to 90%. I found further increase of the number of worms cultured in a plate resulted in decreased efficiency of obtaining suitable hermaphrodites for the experiment because when more than 200 worms are prepared in plates, many worms dig into the agar, making it difficult to find worms that can be used for the experiment. From the same reason, I found it important to use plates that were not cracked or dry. Secondly, to improve the efficiency of obtaining oocyte whose maternal chromosomes were completely released to the polar bodies, I searched for a suitable incubation time after the injection of *klp-18* dsRNA for the RNAi experiment. The maternal chromosomes were removed completely in 9% (2 embryos from 23 dissected worms) when the time after *klp-18* dsRNA injection was less than 31 hours. The success ratio increased to 50% (6 embryos from 12 dissected worms) when the time after injection was 31 hours or more. Based on this result, I moved on to evaluate the efficiency to obtain enucleated embryos by mating *klp-18* hermaphrodites and *emb-27* males. When the incubation time after the *klp-18* dsRNA injection was between 25 and 30 hours, 44% of the embryos (4 embryos from 9 dissected worms) were enucleated. This ratio increased to 83% (5 embryos from 6 dissected worms) when the incubation time was 30 hours or more. The results showed that a high percentage of enucleated embryos could be obtained by adjusting the time from *klp-18* dsRNA injection. After these improvements, I was able to obtain enucleated embryos with high efficiency (Fig. 2D,

Supplemental Movie S4). I did not detect sperm or oocyte pronuclei or any chromosomes inside the embryonic cells at a subsequent stage.

In the enucleated embryo, the centrosomes moved dynamically, which is the main topic of this study that will be analyzed ensuing. This means that the centrosomes can move without the nucleus or chromosomes. Interestingly, the centrosomes duplicated for multiple rounds that appear to correspond to cell cycle. The exact number in the later stage of the enucleated embryo was difficult to determine from the current imaging setup, as the centrosomes became smaller in subsequent cycles. Cytokinesis was impaired, at least in the first several cycles, possibly because of the loss of chromosomes (Bringmann and Hyman, 2005). The invagination of the cell membrane, which was visualized by the GFP::PH probe, became evident in later cycles, but it was difficult to determine whether the cytoplasm was completely separated. Most importantly for this study, the positions of these centrosomes did not overlap but were spread throughout the cell (Fig. 2D), suggesting the existence of a spacing activity. Therefore, the enucleated *C. elegans* embryo is suitable for characterizing the spacing activity of centrosomes independent of the nucleus and spindle. In summary, at least for several cycles of centrosome duplication, cytokinesis was impaired, and sister and non-sister centrosomes shared a common cytoplasm and moved dynamically in the enucleated embryos.

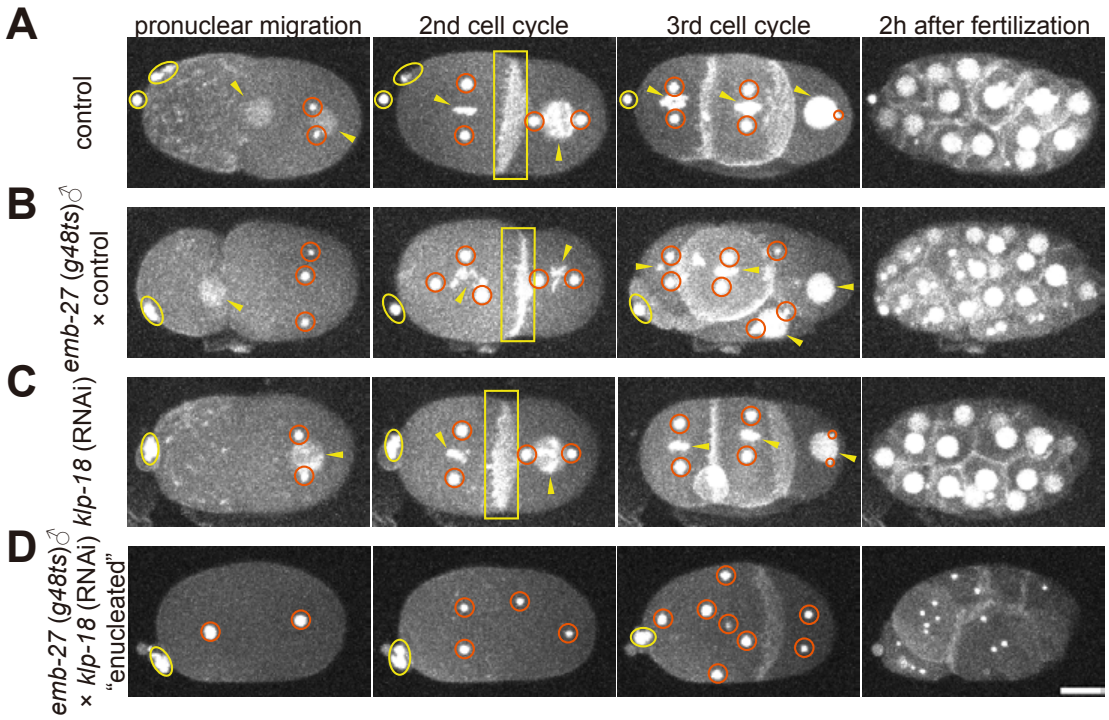

Figure 2: Establishment of enucleated *C. elegans* embryos by genetic manipulation

(A) A time lapse imaging series of an embryo of the control strain (CAL0181) grown at 16 °C, with imaging at 18–22 °C. The reproducibility of the observation was confirmed. (n=5). The red circles indicate centrosomes, the yellow arrowheads indicate pronucleus or nucleus, the yellow oval circles indicate polar body, and the yellow square indicates cell membrane. z-maximum projections. (B) An embryo of the hermaphrodite of the CAL0181 strain mated with males of the CAL0051 strain. Both strains were grown at 25 °C, with imaging at 18–22 °C. (n=5). The red circles indicate centrosomes, the yellow arrowheads indicate pronucleus or nucleus, the yellow oval circle indicates polar body, and the yellow square indicates cell membrane. z-maximum projections. (C) An embryo of the hermaphrodite of CAL0181 with *klp-18* (RNAi) grown at 25 °C after injection, with imaging at 18–22 °C. (n=5). The red circles indicate centrosomes, the yellow arrowheads indicate pronucleus or nucleus, the yellow oval circle indicates polar body,

and the yellow square indicates cell membrane. z-maximum projections. (D) An embryo of the hermaphrodite of CAL0181 with *klp-18* (RNAi) was mated with males of the CAL0051 strain. Both strains were grown at 25 °C, with imaging at 18–22 °C. (n=7). The red circles indicate centrosomes, the yellow circle indicates polar body. z-maximum projections. Scale bar, 10 μm.

A repulsive spacing between sister and non-sister centrosomes was observed in the enucleated embryo

To characterize the force acting between centrosomes, I quantified the change in distance between centrosomes over time. In this study, I focused on a time window corresponding to the 2-cell stage in control embryos with nuclei (Fig. 3). In the enucleated embryo, the cytokinesis fails so the cytoplasm is not divided into two in the "2-cell stage". The four (or more, depending on the number of centrosomes in 1-cell cycle, as explained in the previous section) centrosomes of two sister and non-sister pairs co-exist in the common cytoplasm in this stage. I focused on this stage because it is the earliest stage where I can track the potential interaction between non-sister pairs of the centrosomes. I set the time zero of the time window when I first detected two discrete centrosomes (γ-tubulin) spots for a sister pair of interest after the 2nd centrosome duplication (Fig. 3A). The time window ended when two spots could not be detected or when two spots were again detected in the following round of centrosome duplication.

I compared the distance between sister pairs of the centrosomes in enucleated embryos, as well as those in controls (i.e., embryos with the nuclei) and *zyg-12* (RNAi) embryos (Fig. 3C). At early timepoints in the time window, in control embryos, sister centrosomes slid along the nuclear surface to position themselves at opposite poles of the nucleus (Supplemental Movie S5) (Gönczy et al., 1999). In the enucleated embryo, the sister centrosomes separated at a similar speed to the control embryos, showing that the spacing independent on nucleus (Fig. 3C, Supplemental Movie S7). This result is consistent with previous observations of *zyg-12* (RNAi), in which centrosomes were not associated with nuclei (Malone et al., 2003). At later timepoints, for enucleated

embryos, unlike the control embryo, the separation of the sister centrosomes did not pause at the distance of the nuclear diameter but continued to increase. This behavior can be explained by the loss of association with the nucleus, similar to that observed with *zyg-12* (RNAi) embryos (Supplemental Movie S6). At more later timepoints, in *zyg-12* (RNAi) embryos, the separation of the centrosomes slowed as the centrosomes formed the mitotic spindle, until the centrosomes separated again in anaphase (Fig. 3C). The centrosomes in the enucleated embryo moved in a common cytoplasm, whereas those of the control or *zyg-12* (RNAi) embryos moved in one of the two divided cytoplasms; thus, a direct, quantitative comparison of the centrosome distance between nucleated and enucleated embryos after the cytokinesis is difficult. In summary, centrosomes had the intrinsic ability to separate from their sister centrosomes, independent of the sliding activity along with the nucleus in enucleated embryos. In control embryos, the nucleus tethered sister centrosomes did not separate further until the nuclear envelope breakdown.

An advantage of enucleated embryos is that I can characterize the interaction between non-sister centrosomes that share a common cytoplasm. The distance between the non-sister centrosomes were overall longer than that of sister centrosomes (Fig. 3D). This is reasonable because the initial distance between the non-sister pairs is far longer than that between the sister pairs. The distance between the non-sister centrosomes at time 0 corresponds to the maximum sister centrosome distance in 1 cell cycle before. Interestingly, the distance between the non-sister centrosomes at time 0 tended to be constant depending on the intracellular position of the centrosome. Importantly, even though all centrosomes dynamically move within the embryo, the distances between the non-sisters did not become shorter than the minimal distance between the sister pairs at

each time point (Fig. 3D, 3E). The results indicated that the spacing activity existed not only between sister pairs but also between and non-sister pairs of the centrosomes. Therefore, repulsive spacing activity is intrinsic to the centrosome, possibly because of the interaction between microtubule asters.

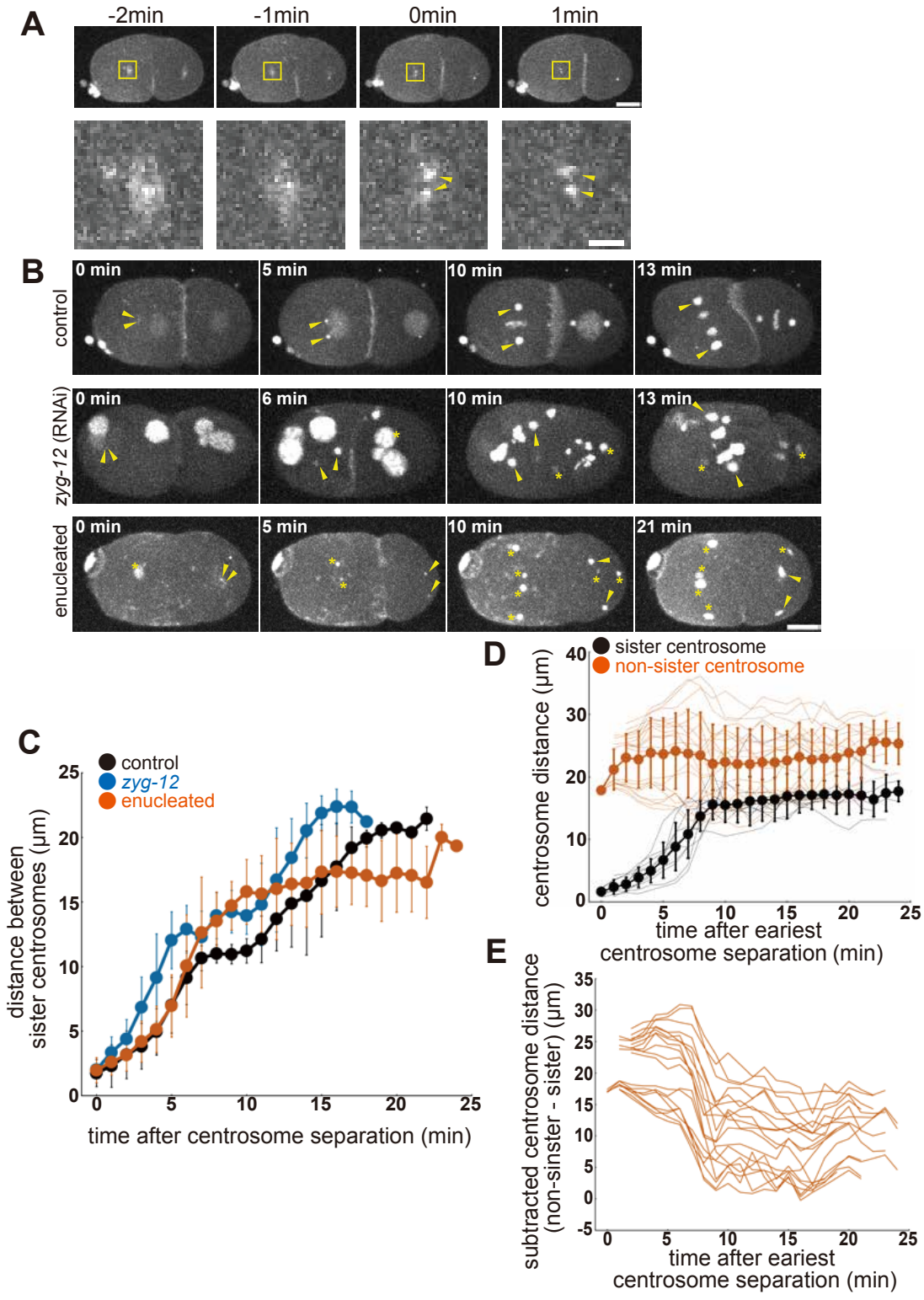

Figure 3: Characterization of centrosome dynamics during the second cell cycle

(A) The definition of time zero in this study. Representative time series images (upper)

and the enlarged images of the yellow box (lower) of an embryo from the enucleated CAL0181 strain. The timepoint when I detected two discrete spots in the cloud of the γ-tubulin signal was defined as time zero. The yellow arrowheads indicate two discrete spots of centrosomes. Upper panels are z-maximum projections. Scale bars, 10 μm for upper panels and 2 μm for lower panels. (B) A time lapse imaging series of an embryo of the control strain (CAL0181), a DE90 strain with *zyg-12* (RNAi) embryo, and an enucleated embryo in the second cell cycle are shown. The yellow arrowheads indicate a pair of sister centrosomes, and the asterisks indicate the other centrosomes in the images. z-maximum projections. Scale bar, 10 μm. (C) The quantification of the distance between sister centrosomes. The mean and S.D. (standard deviation) are shown with the circle and the error bar, respectively. Black, control embryos (eight sister pairs from five embryos). Red, enucleated embryos (ten sister pairs from five embryos). Blue, *zyg-12* (RNAi) embryos (seven sister pairs from five embryos). (D) Distance between the sister- and non-sister-pairs of centrosomes in the enucleated embryo. The distances between the non-sister pairs are calculated for all possible pairs of the non-sisters. Individual samples are shown with thin lines. The mean and S.D. (standard deviation) are shown with the circle and the error bar, respectively. Black, the distance between sister centrosomes. Red, the distance between non-sister centrosomes. (E) The transition of the distance between non-sister centrosomes. Distance between the non-sister-pairs of centrosomes is subtracted by the minimum sister centrosomes distance at each time point in the enucleated embryo. Individual samples are shown with red lines.

Dynein-dependent pulling forces were responsible for the major spacing activity

To obtain insight into the mechanism of the spacing between centrosomes, I searched for genes involved in this activity in the enucleated embryo. Cortical pulling forces, which are the forces pulling the microtubule from force generators located in the cell cortex, have been shown to contribute to centrosome separation in *Drosophila* (Cytrynbaum, 2003). In *C. elegans*, knocking down genes required to generate cortical pulling force (e.g., *gpr-1/2* (RNAi)) impaired the spacing in *zyg-12* knockdown embryos (De Simone et al., 2016). I knocked down *gpr-1/2* in an enucleated embryo to inhibit cortical pulling force, which shortened the distance between the centrosomes (Fig. 4, Supplemental Movie S8). I found significant differences between the enucleated embryos and enucleated embryos with *gpr-1/2* (RNAi) in the values of the distance between the sister centrosomes at the 10-minute timing when the distance between centrosomes in enucleated embryos reaches near saturation ($p<0.01$ by Mann-Whitney *U* test. Mean values for enucleated embryo and enucleated embryo with *gpr-1/2* (RNAi) are 15.8 ± 2.5 μm and 6.9 ± 3.2 μm (mean ± SD), n=10 and 13, respectively). The results indicated that the cortical pulling force mediates the spacing activity. Meanwhile, the centrosomes were separated to some extent in the enucleated *gpr-1/2* (RNAi) embryos. This result was consistent with the incomplete separation of the *zyg-12*; *gpr-1/2* (RNAi) embryos (De Simone et al., 2016). While I could not exclude the possibility that the cortical pulling force was not impaired completely with *gpr-1/2* (RNAi), I expected that different factors were involved in the centrosome spacing activity.

When I knocked down *dhc-1* in the enucleated embryo, the spacing was almost completely blocked for approximately 20 min, which corresponded to the duration of

the cell cycle in the control embryo (Fig. 4, Supplemental Movie S9). *dhc-1* encodes the heavy chain subunit of cytoplasmic dynein and is responsible for all the microtubule pulling forces in *C. elegans* embryos reported to date (Gönczy et al., 1999; Torisawa and Kimura, 2020). I found significant differences between the enucleated embryos with *gpr-1/2* (RNAi) and enucleated embryos with *dhc-1* (RNAi) in the values of the distance between the sister centrosomes at the 10-minute timing ($p<0.01$ By the Mann-Whitney *U* test. Mean values for enucleated embryo with *gpr-1/2* (RNAi) and enucleated embryo with *dhc-1* (RNAi) are 6.9 ± 3.2 μm and 3.1 ± 0.4 μm, n=13 and 12, respectively). Here, I focused on the complete block of the spacing for the first ~20 min, while the spacing after 20 min was analyzed and discussed later in this manuscript. Dynein inhibition impairs the major spacing activity, which occurs within 20 min, almost completely. Therefore, this result suggested that factors other than the cortical pulling force, but depend on dynein, contributed to the spacing.

The cytoplasmic pulling force depends on *dhc-1* but not on *gpr-1/2* and drives centration of the centrosomes and pronuclei, which has been reported in the *C. elegans* embryo (Kimura and Onami, 2005, 2007). I expected that the cytoplasmic pulling force contributed to the spacing. To validate this hypothesis, I knocked down the *dyrb-1* and *gpr-1/2* genes in the enucleated embryo. *dyrb-1* encodes a roadblock subunit of the dynein complex, which is not essential for the motor activity of dynein but is required for organelle transport and centration of the centrosome; therefore, this subunit is necessary for the cytoplasmic pulling force (Kimura and Kimura, 2011). In *dyrb-1*; *gpr-1/2* (RNAi) enucleated embryos, in which the cytoplasmic- and cortical-pulling forces are impaired, but the motor activity of the dynein is intact, the centrosome spacing is essentially blocked, as I observed in the *dhc-1* (RNAi) enucleated

embryo (Fig. 4, Supplemental Movie S11). I found significant differences between the experiment between the enucleated embryos with *gpr-1/2* (RNAi) and enucleated embryos with *gpr-1/2*; *dyrb-1* (RNAi) in the values of the distance between the sister centrosomes at the 10-minute timing ($p<0.01$ By the Mann-Whitney *U* test. Mean values for enucleated embryo with *gpr-1/2* (RNAi) and enucleated embryo with *gpr-1/2* + *dyrb-1* (RNAi) are 6.9 ±3.2 μm and 3.9 ±1.1 μm, n=13 and 12, respectively). From these results, I propose that cortical and cytoplasmic pulling forces are sufficient to provide the spacing between the centrosomes that occurred in the initial ~20 min in the *C. elegans* embryo.

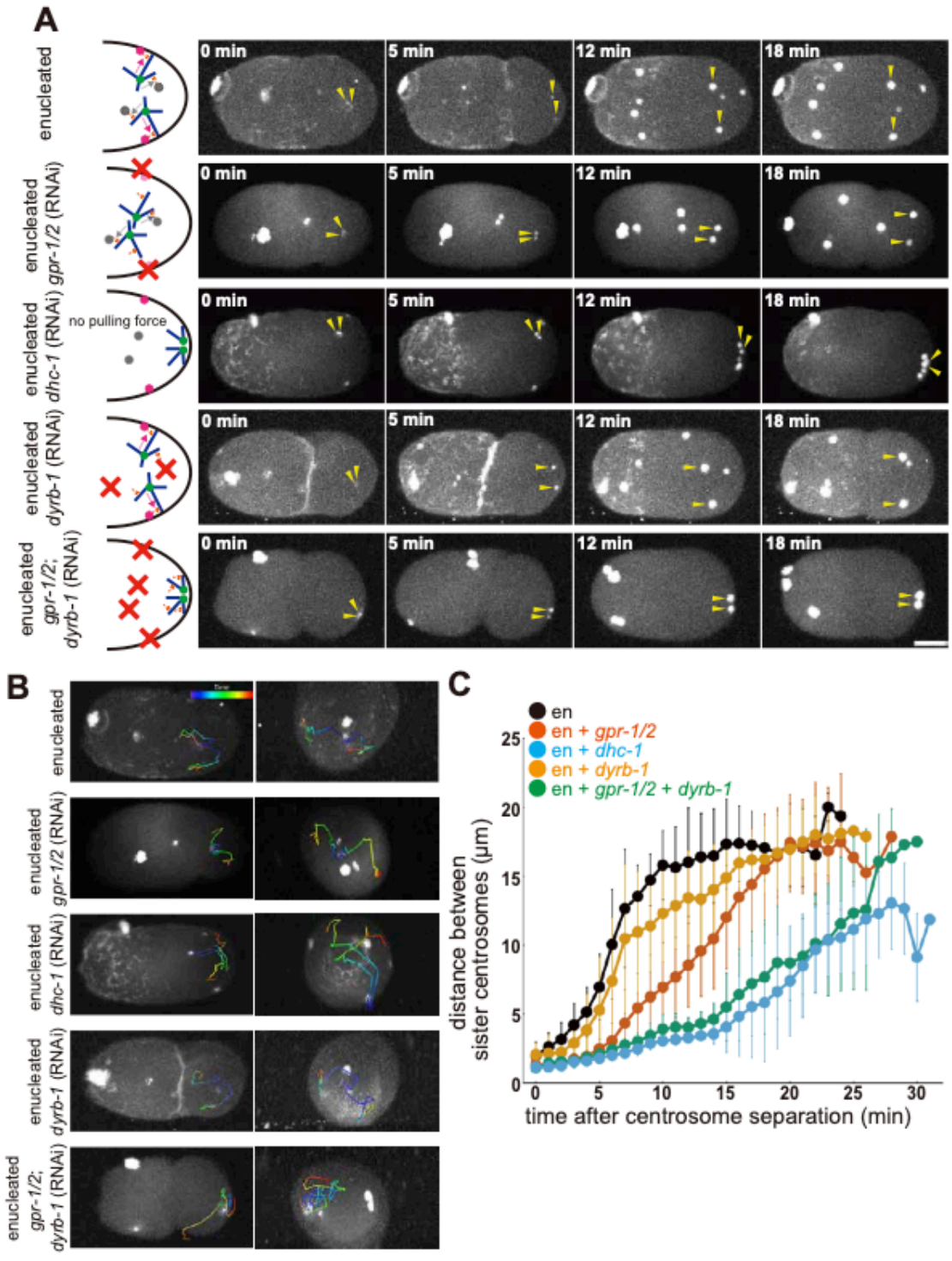

Figure 4: The centrosome spacing activity depends on cortical- and cytoplasmic-pulling forces

(A) Time lapse imaging series of an embryo of an enucleated embryo, and *gpr-1/2* (RNAi),

dhc-1 (RNAi), *dyrb-1* (RNAi), and *dyrb-1;gpr-1/2* (RNAi) enucleated embryos. The left drawing shows each experimental condition. The green circles indicate centrosomes, the blue lines indicate microtubules, the orange indicates dynein, the magenta hexagon indicates a cortical pulling force anchoring complex, the gray circles indicate intracellular organelles. The magenta arrows indicate force by the cortical pulling forces, and the gray arrows indicate force by the cytoplasmic pulling forces, respectively. The yellow arrowheads indicate a pair of sister centrosomes. z-maximum projections. The time zero is when two discrete centrosomes (γ-tubulin) spots were detected for a sister pair of interest after the 2nd centrosome duplication (Described in Fig. 3A). Scale bar, 10 μm. (B) An example of the trajectory of sister centrosomes. The color cylinders show the trajectories for the time that could be tracked for each sample. Snapshots from directly above (left) and from the posterior side of the embryo (right) of a 3D image of the same sample as in (A). The color cylinders indicate the trajectories of the two sister centrosomes. The color bar indicates the progress of time as it shifts from purple to red. Scale bar 5 μm. (C) The quantification of the distance between sister centrosomes. The mean and S.D. (standard deviation) are shown with the circle and the error bar, respectively. Black, enucleated embryos (ten sister pairs from five embryos). Red, *gpr-1/2* (RNAi) enucleated embryos (thirteen sister pairs from five embryos). Blue, *dhc-1* (RNAi) enucleated embryos (twelve sister pairs from five embryos). Yellow, *dyrb-1* (RNAi) enucleated embryos (eleven sister pairs from five embryos). Green, *dyrb-1;gpr-1/2* (RNAi) enucleated embryos (twelve sister pairs from five embryos).

Pulling force competition model as a mechanism for the repulsive spacing between centrosomes in the *C. elegans* embryo

In humans, *Drosophila* and *Xenopus*, other than *C. elegans*, plus-end-directed motors are involved in the centrosome spacing for the mitotic spindle (see Introduction) and are considered to be involved in chromosome-independent spacing by acting on anti-parallel microtubules elongating from the two centrosomes (Deshpande et al., 2021). In contrast, in this study, I found that the minus-end-directed motor, dynein, provided the necessary force for normal separation in the *C. elegans* embryo. Therefore, I aimed to determine how pulling forces mediate repulsive interactions between centrosomes.

Cortical pulling forces can mediate centrosome separation (Cytrynbaum et al., 2003); however, a logical explanation for this is not evident. For example, to separate a pair of centrosomes from the left and right, the left centrosome should have a stronger pull from the left side than from the right and vice versa. How can centrosomes distinguish between the sides to be pulled? A numerical model has been reported to solve this problem (De Simone et al., 2016), in which the authors coupled the cortical pulling force with a cortex flow. In the *C. elegans* 1-cell stage embryo, where the sperm-derived centrosomes separated near the cortex after fertilization, the direction of cytoplasmic flow near the cortex correlated with the direction of movement of each centrosome. Once the centrosomes were on flows directed toward opposite sides, they could be separated (De Simone et al., 2016). While the correlation between the direction of the centrosome movements and the flows has been demonstrated, it is not clear why the centrosomes consistently moved to the opposite side, whereas the flow directions fluctuated. Moreover, the centrosomes were not near the cortex before separation in the later stages, including during the second cell cycle investigated here, and the cortex

flows were specific to the 1-cell stage. Thus, the mechanism to separate the two centrosomes with a pulling force in the non-1-cell stage is undetermined.

Here, I proposed a "pulling force competition model" to explain the centrosome spacing using pulling forces (Fig. 5A). The assumption of the model is that a force generator (in both the cytoplasm and cortex) associates more frequently with a microtubule from a closer centrosome as opposed to that from a distant centrosome. It appears that when the two centrosomes compete for a force generator, the closer one is chosen. This assumption is reasonable because the microtubules grow and shrink dynamically (i.e., dynamic instability), and the probability of reaching a force generator decreases with distance. Intuitively, this model should explain the centrosome spacing, but although the model is simple and reasonable, to the best of our knowledge, the feasibility of the model has not been tested numerically.

I constructed a numerical model that based on the competition model and examined whether this model could reproduce the spacing (Fig. 5B, 5C). Two critical assumptions were made. First, longer microtubules are less frequent than shorter ones. In the model, the probability of a microtubule being longer than the length (l) was modeled as $P(l) = 1 - l/L_0$, were L_0 is the maximum length of the microtubule (see Materials and Methods). Second, a force generator pulls only one microtubule at a time. In 3-dimensional space, force generators in the cytoplasm or the thin layer of the cortex were uniformly distributed, similar to the previous simulation (Kondo and Kimura, 2019). The force generators at the cortex only attach to the tips of the microtubules. Cytoplasmic force generators can attach to both the microtubule tip and the shaft. In this model cell, the centrosomes were positioned indiscriminately as an initial condition and ran the simulation by iterating the processes of growing the microtubule, summing up

the pulling forces, and moving the centrosomes. By using the parameter values from the previous model (Kondo and Kimura, 2019) and by manually adjusting them to align the results with those of the enucleated embryo, the spacing could be reproduced (Fig. 5D). By reducing the pulling force from the cortex, and/or from the cytoplasm, the simulation reproduced tendency observed in the experimental for *gpr-1/2*, *dhc-1*, *dyrb-1* and *gpr-1/2*;*dyrb-1* (RNAi) (Fig. 5D). The numerical simulation results supported the feasibility of the pulling force competition model. Under the condition in which the cortical pulling force is inhibited, the distance between the centrosomes (orange line) decreases at around 17 minutes in the simulation, unlike the experimental results (orange line) at 17 minutes (Fig. 4C), but this may be due to the presence of a flow-dependent mechanism discussed later (Fig. 4C, 5D). The difference between the simulated and experimental results for the condition where the cytoplasmic pulling force is inhibited (yellow line) may be due to the difference in the starting point of the duplicated centrosomes. In the simulation, after the duplication, the centrosomes are distant from the cortex. Therefore, the distance between centrosomes is gradually increased until around the 13 minutes, and as the centrosome is approaching to the cortex, the spacing is accelerated by the cortical pulling force. Inhibition of cytoplasmic pulling force prevents centrosomes centration (Kimura and Kimura, 2011). The experimental results show that the duplicated centrosome is located near the cell cortex. Therefore, even short microtubules can reach the cortex quickly, resulting in rapid spacing by the cortical pulling force.

In addition, the pulling force competition model also reproduced the separation and centration of the centrosomes (Albertson, 1984; Gönczy et al., 1999) associated with the sperm-derived pronucleus of the 1-cell stage embryo (Fig. 5E). For the

simulation with the nucleus, the two centrosomes were connected with an elastic bar with the length of the nuclear diameter (8 μm), by which the centrosomes attract each other when the distance between them exceeds the diameter. This result supports the feasibility of the model for cells with nuclei.

In summary, the centrosome spacing is generated by both cortical and cytoplasmic pulling forces in the experiments using enucleated *C. elegans* embryos. Furthermore, I proposed a pulling forces competition model for the centrosome spacing using these pulling forces. And this model can be explained by a numerical model. The pulling forces competition model can explain how duplicated centrosomes always move in opposite directions in cells with the nucleus.

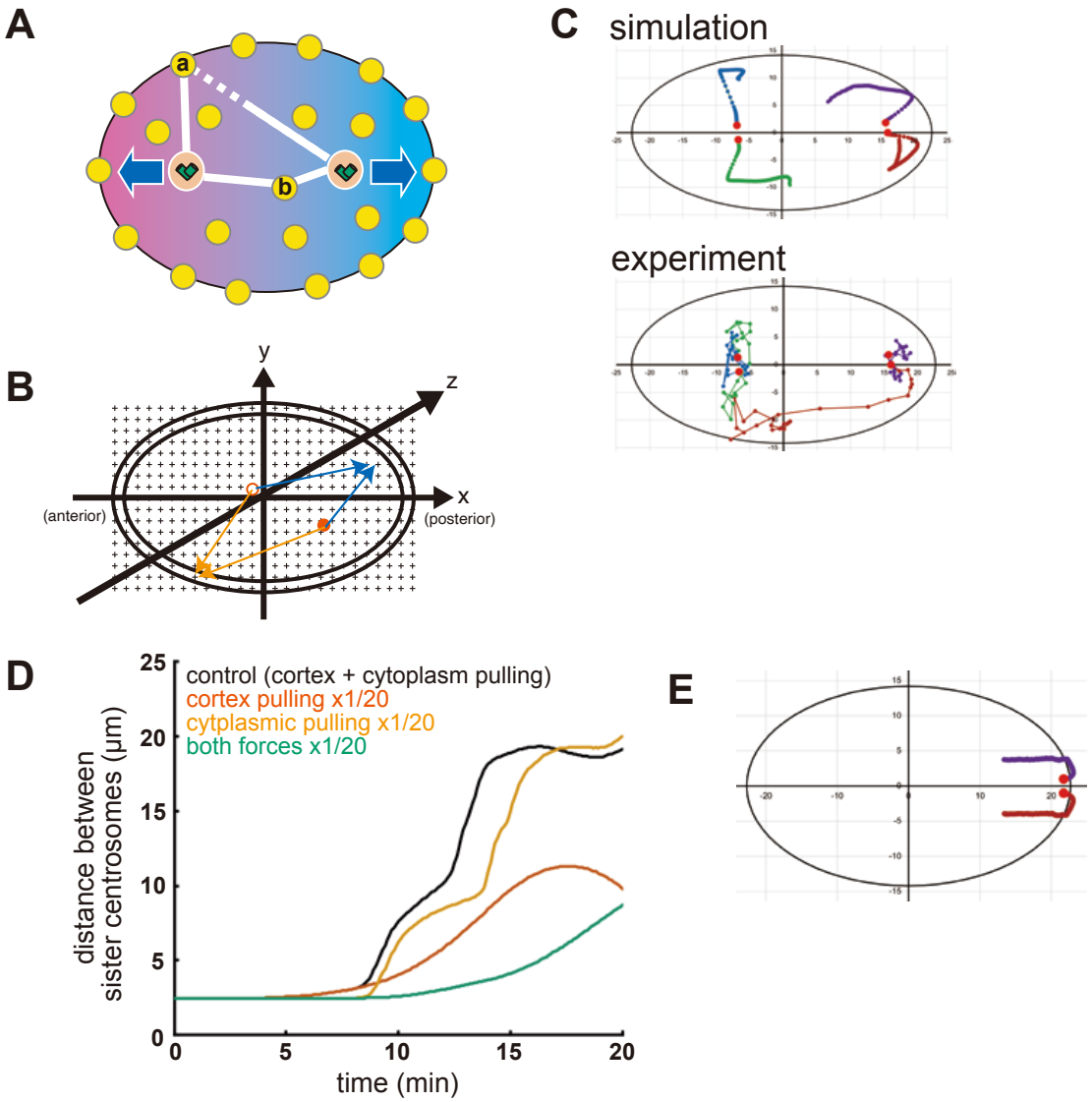

Figure 5: Pulling force competition model

(A) Schematic drawing of the model. Each centrosome (orange circle with two cylinders) are pulled by force generators (yellow circles) at the cell cortex and the cytoplasm. The two key assumptions of this model are: [a] the probability a force generator can pull the centrosome via microtubule depends on the distance to the centrosome. The centrosome located far is unlikely pulled by the force generator, and [b] when a force generator is near enough from multiple centrosomes, it interacts with only one of them. (B) Schematic

drawing of the simulation setup. The ellipsoids represent the cell (the outer layer: the cortex, the inner mass: the cytoplasm). Red circles are the centrosomes. Black crosses on the lattice is the force generators evenly distributed. The force generators at the cortex, or the cytoplasm, pulls the centrosomes depending on the distance between the force generator and each centrosome (orange or blue arrows, respectively). (C) Trajectories of the centrosomes in a representative enucleated embryo (lower) and the simulation with the same initial positions of the four centrosomes (upper). The initial positions of the centrosomes are shown with red circles. The trajectories of the same color indicate the same initial positions. (D) Simulated distance between the sister centrosomes in the simulation in C (black line), and in simulations with reduced cortical pulling forces (red line), with reduced (5%) cytoplasmic pulling forces (yellow line), and with a condition where the both pulling forces are reduced (green line). (E) Simulation for the separation and migration of the centrosomes in the pronuclear migration stage in the wild-type (intact nucleus). The trajectories of the two centrosomes are shown in red and purple lines. The initial positions of the two centrosomes are set near the posterior end of the embryo, and the initial spacing between the centrosomes is 2 μm. The intact nucleus was simulated by restricting the distance between the two centrosomes not exceeding the nuclear diameter (8 μm).

Flow-dependent movements of the centrosomes in the *C. elegans* embryo

In this study so far, I have investigated the mechanism of the spacing between the two centrosomes that occur soon after (<10min) the two spots of the centrosomes were detected. I found that the major spacing which is produced by pulling force competition model occurs in this period is impaired almost completely by *dhc-1* (RNAi). During the course of this analyses, I unexpectedly found a large movement of the centrosomes ~20 min after detecting two centrosomes in the *dhc-1* (RNAi) enucleated embryos (See the colors cylinder shows green to red in Fig. 4B, 4C, Supplemental Movie S9). In the *dhc-1* (RNAi) embryos with nuclei, the centrosomes did not separate during the interphase in the 1-cell stage, and a small spindle-like structure was formed near the cortex, indicating that dynein was responsible for all centrosome movements until the spindle formation stage in normal embryos (Fig. 6A). Although not previously described to my knowledge, I noticed that the centrosomes moved over a large distance in nucleated *dhc-1* (RNAi) embryos, indicating that a large centrosome movement was not specific to the *dhc-1* (RNAi) enucleated embryos (Supplemental Movie S9, Supplemental Movie S12).

A large movement occurs near the time of cytokinesis (in control embryos); therefore, I speculated the involvement of actomyosin, which drives constriction of the contractile ring and accompanying cortical flow toward the equatorial plane. Although cytokinesis does not occur in the enucleated embryo, the cortical flow may move the centrosomes. I could not obtain an enucleated embryo upon knockdown of *nmy-2* encoding non-muscle myosin II that is required for cytoplasmic flow (Munro et al., 2004), possibly because NMY-2 is required for polar body extrusion (Dorn et al., 2010) and lowered the efficiency of oocyte enucleation. Therefore, I knocked down *nmy-*

2 simultaneously with *dhc-1* with RNAi in nucleated embryos. I observed impairment of a large movement of the centrosomes, indicating that this movement is driven by cytoplasmic flow (Fig. 6A, B, Supplemental Movie S13). Differences in distance between centrosomes at 5 minutes after NEBD were tested by the Mann-Whitney *U* test between *dhc-1* and *dhc-1*;*nmy-2* experiments ($p<0.01$. Mean values for *dhc-1* (RNAi) and *dhc-1*; *nmy-2* (RNAi) are 14.9 ± 2.0 μm and 3.9 ± 0.9 μm, n=6 and 5, respectively).

In summary, the cytoplasmic flow drives a large movement of centrosomes in late mitosis that occurs when dynein is inhibited. This flow-dependent movement is considered to be a movement that supports in the centrosome positioning.

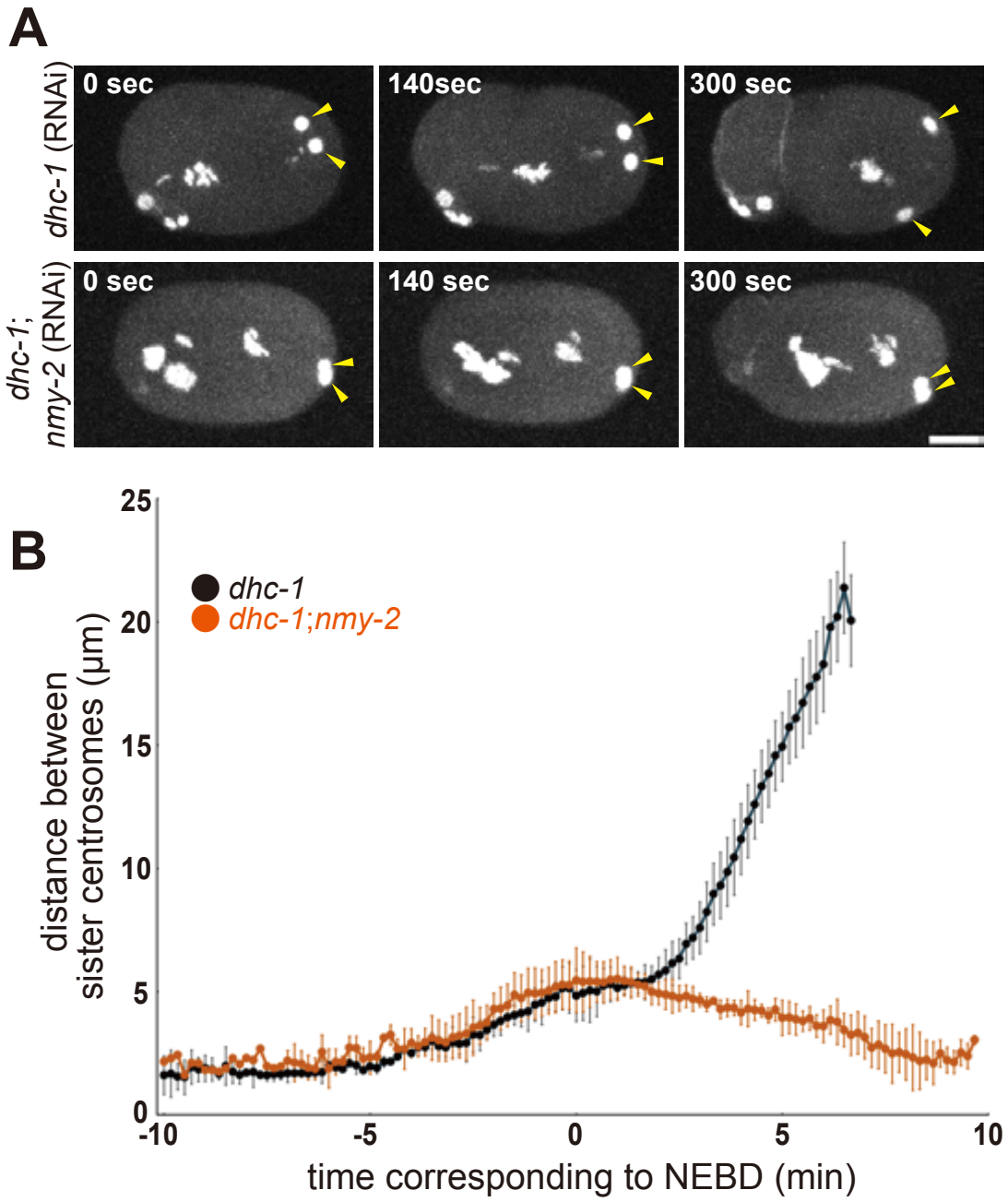

Figure 6: The flow-dependent movement of the centrosomes

(A) Time-lapse imaging series of a *dhc-1* (RNAi) embryo, and a *dhc-1;nmy-2* (RNAi) embryo of the DE90 strain. The yellow arrowheads indicate a pair of sister centrosomes. z-maximum projections. Scale bar, 10 μm. (B) The quantification of the distance between sister centrosomes. The mean and S.D. (standard deviation) are shown by the circle and

the error bar, respectively. Black, *dhc-1* (RNAi) embryos (5 sister pairs from 5 embryos). Red, *dhc-1;nmy-2* (RNAi) embryos (5 sister pairs from 5 embryo).

Two-dimensional self-organized geometry of the centrosomes in *dhc-1* (RNAi) enucleated embryos

In the course of this study, I further found a novel behavior of the centrosomes. In enucleated *dhc-1* (RNAi) embryo, I found that the centrosomes are arranged in a geometrically regular configuration (Fig. 7B). After 6 centrosomes moved dynamically in the *dhc-1* (RNAi) enucleated embryo and dispersed at the end of 2nd cell cycle, 12 centrosomes were assembled in locations near the poles of the embryo at the 3rd cell cycle (Fig. 7A, Supplemental Movie S14). As described in the previous section, flow-dependent movement causes the centrosomes to disperse in the embryo. The time when the centrosomes are farthest apart is 26 min, and the dispersed centrosomes move toward the posterior side from 26 min to 41 min (Fig. 7A). Subsequently, centrosomes are attracted and came closer to each other between 46-56 min (Fig. 7A). Finally, flow-dependent centrosome dispersion was observed around 61 min. (Fig. 7A). These movements repeatedly occurred in each cell cycle for 5/5 embryos. This attractive movement in the *dhc-1* (RNAi) enucleated embryos cannot be currently explained, suggesting a novel mechanism for centrosome movement. In the future, an investigation of the underlying mechanisms would be required to elucidate this movement. In addition, after the centrosomes came close to each other, they did not merge but the centrosomes aligned to a plane with a geometrical regular arrangement (Fig. 7B). Such geometrically regular and planar centrosome configurations of the multiple centrosomes were observed for 2/5 embryos, while in the other 3/5 embryos, the centrosomes started to disperse before they come close enough to judge whether the arrangements were geometrically regular or not. The possible underlying mechanism for

the regular arrangement is completely unknown, which should be investigated in the future.

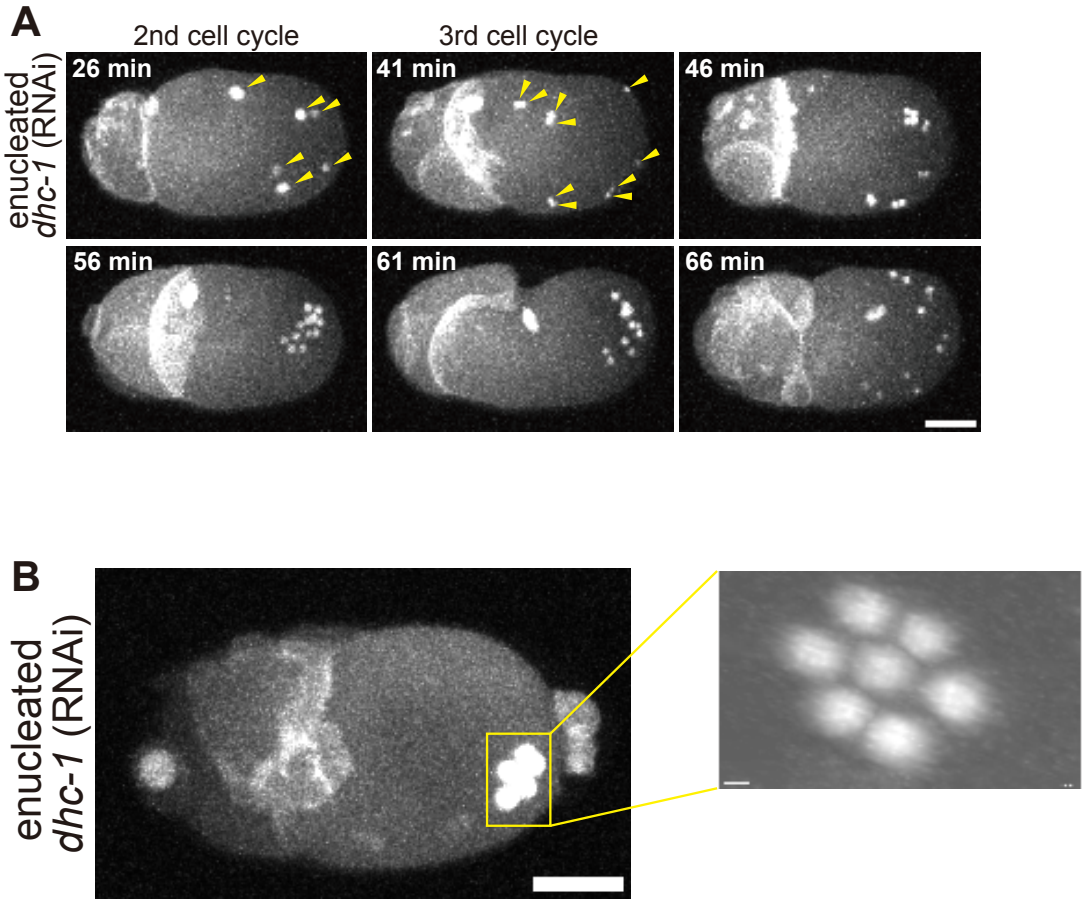

Figure 7: The regular and planar arrangement of the centrosomes in *dhc-1* (RNAi) enucleated embryos

(A) Time-lapse imaging series of a *dhc-1* (RNAi) enucleated embryo after the 2nd cell cycle. (n=5). The yellow arrowheads indicate centrosomes. The time zero is when two discrete centrosomes (γ-tubulin) spots were detected for a sister pair of interest after the 2nd centrosome duplication (Described in Fig. 3A). z-maximum projections. Scale bar, 10 μm. (B) The regular arrangement of the centrosomes. (n=2). (Left) A snapshot of a *dhc-1* (RNAi) enucleated embryo visualized with the Imaris software. (Right) An enlarged image of the centrosomes arranged regularly on a plane. Left panel is z-maximum projection. Scale bars, 10 μm for left panel and 2 μm for right panel.

DISCUSSION

Enucleated *C. elegans* embryos

Chromosomes are essential for cell function because they carry genetic information and constitute a core component of intracellular organelles. Before nuclear envelope breakdown (NEBD), the chromosome forms the cell nucleus, while subsequent to NEBD, it creates the mitotic spindle. The removal of chromosomes from cell has allowed for important modeling for cell biology studies (Goldman and Pollack, 1974). In addition to mechanical removal of the nucleus, such as by centrifugation or microneedles, genetic manipulation can be used to impair the effect of the nuclei. The *gnu* mutant of *Drosophila* revealed a semi-enucleated system for *Drosophila* embryos in which the nucleus does not divide but forms one giant nucleus while the centrosomes continually duplicate and separate (Freeman et al., 1986), so that the separation of the centrosomes is almost entirely independent of the existence of the nuclei (de-Carvalho et al., 2022). In this study, a genetic method to obtain enucleated *C. elegans* embryos was established for the first time by combining previously established methods to remove chromosomes from sperm (Sadler and Shakes, 2000) and oocytes (Segbert et al., 2003). Unlike the *Drosophila gnu* mutant (Freeman et al., 1986), this method completely removes chromosomes from the embryo. I expect the established method to be used in various studies, not limited to centrosome research, because *C. elegans* embryos are widely used model. The current experimental procedure involves multiple steps and is thus laborious. Using the latest methods to inactivate gene function, such as the AID system (Kanemaki et al., 2003; Negishi et al., 2021), I expect that enucleated *C. elegans* embryos can be made more efficiently with

fewer experimental steps. This allows us to perform tests on enucleated embryos and various RNAi experiments.

Chromosome-independent and dynein-dependent spacing between the centrosomes

Using the enucleated *C. elegans* embryo, I demonstrated that the spacing activity independent of the chromosomes exists in the *C. elegans* embryo both before and after NEBD, and between the sister- and non-sister-centrosomes. The chromosome-independent spacing between sister centrosomes before NEBD was previously observed using the *zyg-12* mutant, in which the association between the nucleus and the centrosomes was impaired (Malone et al., 2003; De Simone et al., 2016). In contrast, as the mitotic spindle forms and most of the cells divide in *zyg-12* mutants, the chromosome-independent interaction after NEBD and that for non-sister centrosomes could not be previously addressed. In addition, the nuclei often remain in the cytoplasm between the centrosomes during interphase, which act as obstacles for microtubule growth in these regions. The enucleated embryo is thus a good model system for studying the interaction between centrosomes, independent of the chromosomes (nucleus and mitotic spindle).

I demonstrated that the spacing between the sister and non-sister centrosomes until just before cytokinesis completely impaired the knockdown of dynein (*dhc-1*). This result indicated that direct pushing between the centrosomes, as revealed in *Drosophila* and *Xenopus* (Telley et al., 2012; Nguyen et al., 2014, 2017), did not occur in the *C. elegans* embryo. My observation in *C. elegans* is consistent with the previous researches that the centrosomes rarely moved in *dhc-1* (RNAi) embryo (Gönczy et al., 1999), and the molecules involved in pushing did not impair the

elongation of the mitotic spindle in the *C. elegans* embryo (Powers et al., 2004; Saunders et al., 2007; Lee et al., 2015). Nevertheless, my study using enucleated embryos demonstrated the direct requirement of dynein (*dhc-1*) for the spacing. When chromosomes were present, the defect of the centrosome movement in *dhc-1* (RNAi) condition could be explained by a strong attraction between the centrosomes and the chromosomes.

Pulling force competition model

The major involvement of dynein indicated that the centrosome spacing in *C. elegans* is driven by a pulling force outside of the centrosome pairs but not by a pushing force inside the pairs. This is in contrast to the mechanism of centrosome separation in flies and frogs, where push on the microtubules by kinesin (Telley et al., 2012; Nguyen et al., 2014, 2017). The separation of centrosomes by outward pulling forces is common for centrosome separation before NEBD (Gönczy et al., 1999; Cytrynbaum et al., 2003; De Simone et al., 2016) or spindle elongation (anaphase B) (Grill et al., 2001). However, it has not been determined why the two centrosomes, located adjacent to each other, are pulled in opposite directions. In the case of the mitotic spindle, the spindle itself has bipolarity, and this difference is established upon spindle formation. In other cases, the cell nucleus may amplify the asymmetry by positioning between the centrosomes and hindering the growth of microtubules toward the nucleus (Cytrynbaum et al., 2003; Donoughe et al., 2022). Cortical flow has also been proposed to separate centrosomes (De Simone et al., 2016), but the mechanism to precisely ensure centrosome movement toward the opposite direction has not been clarified.

Here, I propose a simple and reasonable model for centrosome separation using pulling forces without geometric constraints provided by the nucleus or spindle, the pulling force competition model. In this model, I assume that force generators that pull the centrosome via microtubules are evenly distributed throughout the cell cortex and/or cytoplasm. The key assumption is that a force generator has a greater chance of pulling a microtubule connected to the nearer centrosome than the distant centrosome. This is a reasonable assumption, as longer microtubules are rarer than shorter ones as the dynamic microtubules stop growing stochastically (Mitchison and Kirschner, 1984). As a result, the distribution of the microtubule length followed a decay for longer microtubules (Howard, 2001; Kimura et al., 2017). I showed that the pulling force competition model corroborated the spacing dynamics of centrosome pairs in the control and gene knockdown enucleated embryos. Moreover, the model explained the separation and centering of the normal embryo with the nucleus when the centrosomes were tethered on the nuclear surface. Therefore, the pulling force competition model is promising for the centrosome spacing in *C. elegans* embryos and should also be applicable to other cell types and species.

A similar pulling force based mechanism was proposed for the spacing of nuclei in the syncytium embryo of the cricket *Gryllus bimaculatus* (Donoughe et al., 2022), despite the observation of a pushing-based mechanism for similar nuclear spacing in *Drosophila* syncytium embryos (Deshpande et al., 2021). The proposed pulling-based mechanism found in the cricket supports the generality of the mechanism proposed in this study for *C. elegans* embryos. However, further studies are needed to clarify the pulling-based mechanism for the cricket. The involvement of dynein or other pulling force generators has not been demonstrated in this system. The current argument

against the pushing-based mechanism in the cricket is that a numerical simulation (Dutta et al., 2019) does not correspond to some aspects of nuclear migration in the cricket (Donoughe et al., 2022). It is possible that kinesin-5, PRC1, or kinesin-4 may be required for spacing in the cricket. The pulling-based model proposed for the cricket (Donoughe et al., 2022) is similar to that used in this study. Unlike our model, which is independent of the nucleus, the cricket model assumed occlusion of the microtubule "cloud" by the nucleus as the primary driving force. In *Drosophila*, the spacing of the centrosomes in the syncytium is independent of the nucleus (de-Carvalho et al., 2022), and this may also be the case for the cricket. In this scenario, our pulling force competition model, which does not require nuclei for the spacing, would be more suitable, even for the cricket. Finally, in contrast to the cricket model, in which an occlusion between the microtubule "clouds" was assumed without mechanistic bases, our pulling force competition model assumes competition based on the reasonable length distribution of the microtubule (i.e., longer microtubules are rare). In this regard, I believe that the pulling force competition model is a more widely applicable model with a more reasonable mechanistic basis.

The pulling force competition is a reasonable model for initial separation of the centrosomes when the microtubule asters are in the initial phase of growing. The key assumption of the model was that longer microtubules are rare. Qualitatively, this condition should be fulfilled consistently. Quantitatively, in contrast, the difference in the frequency of a long and short microtubule is expected to decrease when the microtubule asters grow. For the centrosomes to achieve the robust spacing after the growth of the microtubule asters, it may require other mechanisms. Numerical modeling

of the spacing should be a powerful tool for investigating a robust mechanism in the future.

Myosin-dependent centrosome movement

I observed large movement of the centrosomes during the cytokinesis period in normal (nucleated) embryos when knockdown dynein (*dhc-1*). This was unexpected because previous studies described that the centrosomes do not move upon knockdown of dynein (*dhc-1*) in the *C. elegans* embryo (Gönczy et al., 1999). To my knowledge, the later stages of embryogenesis have not been included in previous studies, and there are many interesting phenotypes in *dhc-1* knockdown embryos. I observed dynamic centrosome movement upon the *dhc-1* (RNAi) in the nucleated embryo.

A large movement of the centrosomes in the *dhc-1* (RNAi) embryo coincided with the timing of cytokinesis; therefore, I expected the involvement of cytoplasmic flow coupled with the cytokinesis (White and Borisy, 1983; Khaliullin et al., 2018) because a large centrosome movement was impaired when the non-muscle myosin *nmy-2* was knocked down. I confirmed that cytoplasmic flow occurred in *dhc-1* (RNAi). The involvement of cytoplasmic streaming in centrosome movement in *C. elegans* embryos was proposed in a previous study, in which the centrosomes moved along the cortex in *zyg-12* (RNAi) embryos in a *nmy-2*-dependent manner immediately after fertilization (De Simone et al., 2016). This movement of the centrosome immediately after fertilization may not be necessarily caused by cytoplasmic streaming, because *nmy-2* (RNAi) impairs cortical pulling forces (Redemann et al., 2010). Therefore, the centrosome movement behavior in *zyg-12*; *nmy-2* (RNAi) (De Simone et al., 2016) can be explained by defects in the cortical pulling force. In support of this idea, centrosomes

in *dhc-1* (RNAi) embryos moved little after fertilization, although cytoplasmic flow was observed.

Geometric-organization of the centrosome position in *dhc-1* (RNAi) enucleated embryos

Surprisingly, I found that centrosomes attract each other in the *dhc-1* (RNAi) enucleated embryos. Furthermore, when centrosomes are gathered, they adopt a geometrically regular arrangement inside the cell that to my knowledge, is previously undocumented. The mechanism underlying this structure is also unclear, as is the method by which centrosomes attract each other over such a long-range without dynein, and assemble at the pole of the embryo as opposed to the center. It is also undetermined how the centrosomes adopt a regular arrangement instead of simply aggregating and why they are aligned on a plane rather than in a 3D structure. Therefore, to address these questions, it is required to clarify whether centrosomes are gathered passively or actively by further experiments. Furthermore, detailed characterization of the structure using a finer resolution, such as that of EM imaging, is also required to clarify these issues. In addition, a modeling approach that narrows down the possible forces acting between centrosomes would be helpful. This is a subject for future research.

CONCLUSION

We propose a simple and reasonable pulling force competition model for the centrosome spacing independent of the nucleus or spindle in *C. elegans* embryos. The mechanism is expected to function in other cell types and organisms in combination with repulsive pushing between centrosomes using anti-parallel microtubules. The spacing of centrosomes by the competition model may play a part in the rapid placement of centrosomes during the developmental process. This could be applicable to species with asters formed only by short microtubules. The model was proposed based on experiments using enucleated *C. elegans* embryos. The *C. elegans* embryo is a powerful model for cell and developmental biology, and the experimental setup must be sufficiently powerful to address other biological questions.

MATERIALS AND METHODS

Worm strains and RNAi

The *C. elegans* strains used in this study are listed in Table 1. The DE90 strain (*tbg-1*::*GFP* ; *GFP*::*histone H2B* ; *GFP*::*PH*) was used to obtain embryos with nuclei (*zyg-12*, *dhc-1* and *dhc-1*;*nmy-2* RNAi experiments). The strains were maintained under standard conditions (Brenner, 1974). Knockdown of *zyg-12*, *klp-18, gpr-1/2, dhc-1, dyrb-1*, and *nmy-2* genes was performed using the injection RNAi method as previously described (Kimura and Kimura, 2011). For the double or triple RNAi experiments, the RNA was mixed 1:1 or 1:1:1 and injected into the worm. The concentrations of dsRNA for *klp-18* was 18 or 21μg/μl, *gpr-1/2* was 15 or 19μg/μl, for *dhc-1* was 19μg/μl, and for *dyrb-1* was 13μg/μl. To efficiently obtain the *klp-18* phenotype (enucleated embryos), observation was started <24h after injection. Observations were also conducted <26h after double knockdown and <30h after the triple knockdown. The worms were incubated at 25 °C for <16h before observation (*zyg-12*, *dhc-1* and *dhc-1*;*nmy-2* RNAi experiments).

Production of enucleated embryos

Enucleated embryos were produced using the following procedure. First, on Day 1, a preculture was started to obtain two young adult worms of the CAL0181 and CAL0051 strains the following day. On Day 2, 15 CAL0051 and 10 CAL0181 young adults were separately moved onto new 6 cm (diameter) NGM plates with *E. coli,* and the plates were cultured at 16 °C, an unrestrictive temperature. 24h later, on Day 3, the worms were removed from the plate, and only the embryos that had been laid in the last 24 h

remained on the plate. Cultures were maintained at 16 °C. On Day 4, 24h after the procedures on Day 3, the plates were transferred from 16 °C to 25 °C, which is the restrictive temperature. On Day 5, 24h after the procedures on Day 4, 25 CAL0181 young adults were selected (hermaphrodites with a black intestine and vulva) and injected with *klp-18* dsRNA. After the injection, culturing on the NGM plate continued, with five times the number of CAL0051 males added. A 3.5 cm NGM plate was used for mating. Scratched or dried plates were avoided to prevent the worms from digging inside. Finally, on Day 6, 24h or more after the injection, the worms were dissected, and the embryo was observed under a fluorescence microscope.

Microscopic observation

The localization of fluorescent proteins was observed using a two-photon excitation spinning-disk confocal microscope (CSU-MP; Yokogawa Electric, Tokyo, Japan) (Otomo et al., 2015; Kamada et al., 2022) equipped with an ALCOR920-2 (Spark Lasers, Martillac, France) and an EM-CCD camera (iXon; Andor, Belfast, UK) mounted on an IX71 microscope (Olympus, Tokyo, Japan) and controlled using NIS-elements software (Nikon, Tokyo, Japan). The details of the system and examination of phototoxicity will be published elsewhere (in preparation). The dissected worm embryos were attached to polylysine-coated cover glass and mounted on a microscope. Using a 40× objective lens with 2× intermediate magnification, 61 or 71 images were taken at 0.5 μm intervals on the z-axis. Time-lapse images were collected at 1 min intervals for 1, 2 h or during the 2-cell stage. In *dhc-1* (RNAi) and *dhc-1*;*nmy-2* (RNAi) experiment, 41 images were taken at 0.5 μm intervals on the z-axis. Time-lapse images were collected at 10 second intervals during 1-cell stage. Under these microscope

conditions, *C. elegans* embryos were confirmed to hatch. The captured images were analyzed using ImageJ or Imaris software.

Analysis of centrosome distance

The distance between the centrosomes was analyzed using Imaris 3D analysis software. The signals of the centrosomes were tracked manually using the spot tracking mode. The centroid coordinates of the signal of the centrosomes were calculated by the software. From the calculated coordinates, the distance between the centrosome was calculated using the Pythagorean theorem. For WT, *zyg-12* (RNAi), and enucleated embryos, the centrosomes (Fig. 3A), which split in two at the 2nd cell cycle, were tracked until the signal could be traced or until the next replication took place. For *dhc-1* (RNAi) and *dhc-1*;*nmy-2* (RNAi) experiments, centrosome signals during the 1-cell stage were tracked until they could be traced.

Statistical analysis

The distances between the centrosomes were statistically compared by the Mann-Whitney *U* test. The Mann-Whitney *U* test was performed on the two experimental groups of interest. The calculation was performed using Microsoft Excel software.

Numerical simulation of the pulling force competition model

The settings of the previous simulation (Kondo and Kimura, 2019) were modified to model the embryo as a 3D ellipsoid with a long axis of 45.4 μm and two short axes of 28.2 μm based on the size of the actual embryo. As in the previous simulation, “force generation points” were distributed throughout the cytoplasm and the cortex (2 μm thick

layer) at the vertices of a simple cubic lattice with 1-μm intervals. When a force generation point was associated with a microtubule elongating from a centrosome, the point pulled the centrosome with a defined force (Table 2). The probability of the point associated with the microtubule was defined by the elapsed time (t [s]) and the distance between the point and centrosome (l [μm]) as $P(l,t) = 1 - 120 \times l/t$. ($P(l,t) = 0$ when $l > t/120$ [μm]). Whether the force generator pulls the centrosome for that step (6s) is determined by generating a random number between 0 and 1 and comparing the number with the probability. If a force generator can associate with multiple centrosomes (for example, namely #1 and #2 with the probability of P_1 and P_2, respectively), first the probability of pulling either centrosome was calculated as $1-(1-P_1)\times(1-P_2)$, and comparing it with another random number. Next, the centrosome was determined: it pulls centrosome #1 with the probability of $P_1/(P_1+P_2)$ and #2 with that of $P_2/(P_1+P_2)$. This step is described as follows; a force generator is are more likely to interact and pull the nearer centrosome. A force generator can interact/pull only one centrosome at a time. Therefore, the centrosomes will compete for the force generator. The probability of a force generator to associate with the centrosome, and that of a centrosome win over another centrosome for the force generator, depends on the distance between the force generator and each of the centrosomes. This step represents the competition. After the forces acting on each centrosome were summed, the velocity of the movement was calculated as $\vec{v} = \vec{F}/k_d$, where $\vec{F}$, k_d, and $\vec{v}$ are the force vector, drag coefficient, and velocity vector, respectively. The positions of the centrosomes at the next step were then calculated as $\overrightarrow{r_{t+\Delta t}} = \vec{r_t} + \vec{v} \times \Delta t$, where $\vec{r_t}$ and $\overrightarrow{r_{t+\Delta t}}$ are the position vectors of the centrosomes at time t and $t+\Delta t$, respectively, and

Δt is the time interval. This calculation was repeated for the defined steps starting from the initial positions of the centrosomes.

For the case where the centrosomes were tethered to the surface of the nucleus, we added an additional process after each step to apply an elastic force, $\overrightarrow{F_1} = -k_s(\overrightarrow{r_1} - \overrightarrow{r_2})$ if $R > |\overrightarrow{r_1} - \overrightarrow{r_2}|$ to maintain the distance between the centrosomes at R or shorter. Here, $\overrightarrow{r_1}$ and $\overrightarrow{r_2}$ are the position vectors of the centrosome that the force applied and that of the other centrosome, respectively. k_s is the elastic constant and R is the diameter of the nucleus (8 μm).

The simulation was coded using MATLAB, and the codes are available upon request.

REFERENCES

Albertson, D.G. 1984. Formation of the first cleavage spindle in nematode embryos. *Dev Biol*. 101:61–72. doi:10.1016/0012-1606(84)90117-9.

Baker, J., W. Theurkauf, and G. Schubiger. 1993. Dynamic changes in microtubule configuration correlate with nuclear migration in the preblastoderm Drosophila embryo. *J Cell Biol*. 122:113–121. doi:10.1083/jcb.122.1.113.

Brenner, S. 1974. The genetics of Caenorhabditis elegans. *Genetics*. 77:71–94.

Bringmann, H., and A.A. Hyman. 2005. A cytokinesis furrow is positioned by two consecutive signals. *Nature*. 436:731–734. doi:10.1038/nature03823.

Brust-Mascher, I., G. Civelekoglu-Scholey, M. Kwon, A. Mogilner, and J.M. Scholey. 2004. Model for anaphase B: role of three mitotic motors in a switch from poleward flux to spindle elongation. *Proc Natl Acad Sci Usa*. 101:15938–15943. doi:10.1073/pnas.0407044101.

de-Carvalho, J., S. Tlili, L. Hufnagel, T.E. Saunders, and I.A. Telley. 2022. Aster repulsion drives short-ranged ordering in the Drosophila syncytial blastoderm. *Development*. 149:dev199997. doi:10.1242/dev.199997.

Chaaban, S., S. Jariwala, C.Hsu, S. Redemann, J. Kollman, T. Müller-Reichert, D. Sept, K. H, Bui, and G. J. Brouhard. 2018. The structure and dynamics of *C. elegans* tubulin reveals the mechanistic basis of microtubule growth. *Dev Cell*. 47:191-204. doi:10.1016/j.devcel.2018.08.023.

Cheerambathur, D.K., I. Brust-Mascher, G. Civelekoglu-Scholey, and J.M. Scholey. 2008. Dynamic partitioning of mitotic kinesin-5 cross-linkers between microtubule-bound and freely diffusing states. *J Cell Biol*. 182:429–436. doi:10.1083/jcb.200804100.

Cytrynbaum, E.N., J.M. Scholey, and A. Mogilner. 2003. A force balance model of early spindle pole separation in Drosophila embryos. *Biophys J*. 84:757–769. doi:10.1016/s0006-3495(03)74895-4.

Deneke, V.E., A. Puliafito, D. Krueger, A.V. Narla, A. De Simone, L. Primo, M. Vergassola, S. De Renzis, and S. Di Talia. 2019. Self-Organized Nuclear Positioning Synchronizes the Cell Cycle in *Drosophila* Embryos. *Cell*. 117:925-941. doi:10.1016/j.cell.2019.03.007.

Deshpande, O., J. de-Carvalho, D.V. Vieira, and I.A. Telley. 2021. Astral microtubule cross-linking safeguards uniform nuclear distribution in the Drosophila syncytium. *J Cell Biol*. 221:e202007209. doi:10.1083/jcb.202007209.

De Simone, A., F. Nédélec, and P. Gönczy. 2016. Dynein transmits Polarized Actomyosin Cortical Flows to Promote Centrosome Separation. *Cell Rep*. 14:2250–2262. doi:10.1016/j.celrep.2016.01.077.

Dogterom, M., and B. Yurke. 1997. Measurement of the force-velocity relation for growing microtubules. *Science*. 278:856-860. doi:10.1126/science.278.5339.856.

Donoughe, S., J. Hoffmann, T. Nakamura, C.H. Rycroft, and C.G. Extavour. 2022. Nuclear speed and cycle length co-vary with local density during syncytial blastodem formation in a cricket. *Nat Commun*. 13;3889. doi:10.1038/s41467-022-31212-8.

Dorn, J.F., L. Zhang, V. Paradis, D. Edoh-Bedi, S. Jusu, P.S. Maddox, and A.S. Maddox. 2010. Actomyosin Tube Formation in Polar Body Cytokinesis Requires Anillin in *C. elegans*. *Curr Biol*. 20:2046–2051. doi:10.1016/j.cub.2010.10.030.

Dutta, S., N.J.-V. Djabrayan, S. Torquato, S.Y. Shvartsman, and M. Krajnc. 2019. Self-Similar Dynamics of Nuclear Packing in the Early Drosophila Embryo. *Biophys J*. 117:743–750. doi:10.1016/j.bpj.2019.07.009.

Elric, J., and S. Etienne-Manneville. 2014. Centroeome positioning in polarized cells: Common themes and variations. *Exp Cell Res*. 328:240-248. doi:10.1016/j.yexcr.2014.09.004.

Freeman, M., C. Nüsslein-Volhard, and D.M. Glover. 1986. The dissociation of nuclear and centrosomal division in gnu, a mutation causing giant nuclei in Drosophila. *Cell*. 46:457–468. doi:10.1016/0092-8674(86)90666-5.

Goldman, R.D., and R. Pollack. 1974. Chapter 9 Uses of Enucleated Cells. *Methods Cell Biol*. 8:123–143. doi:10.1016/s0091-679x(08)60448-3.

Gönczy, P., S. Pichler, M. Kirkham, and A.A. Hyman. 1999. Cytoplasmic dynein is required for distinct aspects of MTOC positioning, including centrosome separation, in the one cell stage Caenorhabditis elegans embryo. *J Cell Biol*. 147:135–150. doi:10.1083/jcb.147.1.135.

Grill, S.W., and A.A. Hyman. 2005. Spindle positioning by cortical pulling forces. *Dev Cell*. 8:461-466. doi:10.1016/j.devcel.2005.03.014.

Grill, S.W., P. Gönczy, E.H. Stelzer, and A.A. Hyman. 2001. Polarity controls forces governing asymmetric spindle positioning in the Caenorhabditis elegans embryo. *Nature*. 409:630–633. doi:10.1038/35054572.

Howard, J. 2001. Mechanics of motor proteins and the cytoskeleton. Sinauer Associates, Inc.

Kamada, T., K. Otomo, T. Murata, K. Nakata, S. Hiruma, R. Uehara, M. Hasebe, and T. Nemoto. 2022. Low-invasive 5D visualization of mitotic progression by two-photon excitation spinning-disk confocal microscopy. *Sci Rep*. 12:809. doi:10.1038/s41598-021-04543-7.

Kanemaki, M., A. Sanchez-Diaz, A. Gambus, and K. Labib. 2003. Functional proteomic identification of DNA replication proteins by induced proteolysis in vivo. *Nature*. 423:720–724. doi:10.1038/nature01692.

Kanesaki, T., C.M. Edwards, U.S. Schwarz, and J. Grosshans. 2011. Dynamic ordering of nuclei in syncytial embryos: a quantitative analysis of the role of cytoskeletal networks. *Integr Biol*. 3:1112–1119. doi:10.1039/c1ib00059d.

Khaliullin, R.N., R.A. Green, L.Z. Shi, J.S. Gomez-Cavazos, M.W. Berns, A. Desai, and K. Oegema. 2018. A positive-feedback-based mechanism for constriction rate acceleration during cytokinesis in Caenorhabditis elegans. *eLife*. 7:91. doi:10.7554/elife.36073.

Kimura, A., and S. Onami. 2005. Computer simulations and image processing reveal length-dependent pulling force as the primary mechanism for *C. elegans* male pronuclear migration. *Dev Cell*. 8:765–775. doi:10.1016/j.devcel.2005.03.007.

Kimura, A., and S. Onami. 2007. Local cortical pulling-force repression switches centrosomal centration and posterior displacement in *C. elegans*. *J Cell Biol*. 179:1347–1354. doi:10.1083/jcb.200706005.

Kimura, A., and S. Onami. 2010. Modeling microtubule-mediated forces and centrosome positioning in Caenorhabditis elegans embryos. *Methods Cell Biol*. 97:437–453. doi:10.1016/s0091-679x(10)97023-4.

Kimura, K., and A. Kimura. 2011. Intracellular organelles mediate cytoplasmic pulling force for centrosome centration in the Caenorhabditis elegans early embryo. *Proc Natl Acad Sci USA*. 108:137–142. doi:10.1073/pnas.1013275108.

Kimura, K., A. Mamane, T. Sasaki, K. Sato, J. Takagi, R. Niwayama, L. Hufnagel, Y. Shimamoto, J.-F. Joanny, S. Uchida, and A. Kimura. 2017. Endoplasmic-reticulum-mediated microtubule alignment governs cytoplasmic streaming. *Nat Cell Biol*. 19:399–406. doi:10.1038/ncb3490.

Kondo, T., and A. Kimura. 2019. Choice between 1- and 2-furrow cytokinesis in Caenorhabditis elegans embryos with tripolar spindles. *Mol Biol Cell*. 30:2065–2075. doi:10.1091/mbc.e19-01-0075.

Lee, K.Y., B. Esmaeili, B. Zealley, and M. Mishima. 2015. Direct interaction between centralspindlin and PRC1 reinforces mechanical resilience of the central spindle. *Nat Commun*. 6:7290. doi:10.1038/ncomms8290.

Malone, C.J., L. Misner, N.L. Bot, M.-C. Tsai, J.M. Campbell, J. Ahringer, and J.G. White. 2003. The *C. elegans* hook protein, ZYG-12, mediates the essential attachment between the centrosome and nucleus. *Cell*. 115:825–836. doi:10.1016/s0092-8674(03)00985-1.

Meraldi, P. 2016. Centrosomes in spindle organization and chromosome segregation: a mechanistic view. *Chromosome Res*. 24:19–34. doi: 10.1007/s10577-015-9508-2.

Mitchison, T., and M. Kirschner. 1984. Dynamic instability of microtubule growth. *Nature*. 312:237–242.

Mogilner, A., R. Wollman, G. Civelekoglu-Scholey, and J. Scholey. 2006. Modeling mitosis. *Trends Cell Biol*. 16:88-96. doi:10.1016/j.tcb.2005.12.007.

Munro, E., J. Nance, and J.R. Priess. 2004. Cortical flows powered by asymmetrical contraction transport PAR proteins to establish and maintain anterior-posterior polarity in the early *C. elegans* embryo. *Dev Cell*. 7:413–424. doi:10.1016/j.devcel.2004.08.001.

Negishi, T., S. Kitagawa, N. Horii, Y. Tanaka, N. Haruta, A. Sugimoto, H. Sawa, K. Hayashi, M. Harata, and M.T. Kanemaki. 2021. The auxin-inducible degron 2 (AID2) system enables controlled protein knockdown during embryogenesis and development in Caenorhabditis elegans. *Genetics*. doi:10.1093/genetics/iyab218.

Nguyen, P.A., C.M. Field, and T.J. Mitchison. 2017. Prc1E and Kif4A control microtubule organization within and between large *xenopus* egg asters. *Mol Biol Cell*. 29:mbc.E17-09-0540. doi:10.1091/mbc.e17-09-0540.

Nguyen, P.A., A.C. Groen, M. Loose, K. Ishihara, M. Wühr, C.M. Field, and T.J. Mitchison. 2014. Spatial organization of cytokinesis signaling reconstituted in a cell-free system. *Science*. 346:244–247. doi:10.1126/science.1256773.

O'Connell, K.F. 1999. The centrosome of the early *C. elegans* embryo: inheritance, assembly, replication, and developmental roles. *Curr Top Dev Biol*. 49:365–384. doi:10.1016/s0070-2153(99)49018-0.

Oegema, K., and T.J. Mitchison. 1997. Rappaport rules: Cleavage furrow induction in animal cells. *Proc Natl Acad Sci USA*. 94:4817-4820. doi:10.1073/pnas.94.10.4817.

Otomo, K., T. Hibi, T. Murata, H. Watanabe, R. Kawakami, H. Nakayama, M. Hasebe, and T. Nemoto. 2015. Multi-point scanning two-photon excitation microscopy by utilizing a high-peak-power 1042-nm laser. *Anal Sci*. 31:307–313. doi:10.2116/analsci.31.307.

Powers, J., D.J. Rose, A. Saunders, S. Dunkelbarger, S. Strome, and W.M. Saxton. 2004. Loss of KLP-19 polar ejection force causes misorientation and missegregation

of holocentric chromosomes. *J Cell Biol*. 166:991–1001. doi:10.1083/jcb.200403036.

Redemann, S., J. Pecreaux, N.W. Goehring, K. Khairy, E.H.K. Stelzer, A.A. Hyman, and J. Howard. 2010. Membrane invaginations reveal cortical sites that pull on mitotic spindles in one-cell *C. elegans* embryos. *PLoS One*. 5:e12301. doi:10.1371/journal.pone.0012301.

Reinemann, D.N., E.G. Sturgill, D.K. Das, M.S. Degen, Z. Vörös, W. Hwang, R. Ohi, and M.J. Lang. 2017. Collective Force Regulation in Anti-parallel Microtubule Gliding by Dimeric Kif15 Kinesin Motors. *Curr Biol*. 27:2810-2820.e6. doi:10.1016/j.cub.2017.08.018.

Rios, R.M., and M. Bornens. 2003. The Golgi apparatus at the cell centre. *Curr Opin Cell Biol*. 15:60-66. doi:10.1016/S0955-0674(02)00013-3.

Sadler, P.L., and D.C. Shakes. 2000. Anucleate Caenorhabditis elegans sperm can crawl, fertilize oocytes and direct anterior-posterior polarization of the 1-cell embryo. *Development*. 127:355–366.

Saunders, A.M., J. Powers, S. Strome, and W.M. Saxton. 2007. Kinesin-5 acts as a brake in anaphase spindle elongation. *Curr Biol*. 17:R453-4. doi:10.1016/j.cub.2007.05.001.

Segbert, C., R. Barkus, J. Powers, S. Strome, W.M. Saxton, and O. Bossinger. 2003. KLP-18, a Klp2 kinesin, is required for assembly of acentrosomal meiotic spindles in Caenorhabditis elegans. *Mol Biol Cell*. 14:4458–4469. doi:10.1091/mbc.e03-05-0283.

Silkworth, W.T., I.K. Nardi, R. Paul, A. Mogilner, and D. Cimini. 2011. Timing of centrosome separation is important for accurate chromosome segregation. *Mol Biol Cell*. 23:401-411. doi:10.1091/mbc.e11-02-0095.

Tanenbaum, M.E., and R.H. Medema. 2010. Mechanisms of Centrosome Separation and Bipolar Spindle Assembly. *Dev Cell*. 19:797–806. doi: 10.1016/j.devcel.2010.11.011.

Tang, N., and W.F. Marshall. 2012. Centrosome positioning in vertebrate development.

J Cell Sci. 21:4915-4961. doi: 10.1242/jcs.038083.

Tao, L., A. Mogilner, G. Civelekoglu-Scholey, R. Wollman, J. Evans, H. Stahlberg, and J.M. Scholey. 2006. A Homotetrameric Kinesin-5, KLP61F, Bundles Microtubules and Antagonizes Ncd in Motility Assays. *Curr Biol*. 16:2293–2302. doi:10.1016/j.cub.2006.09.064.

Telley, I.A., I. Gáspár, A. Ephrussi, and T. Surrey. 2012. Aster migration determines the length scale of nuclear separation in the Drosophila syncytial embryo. *J Cell Biol*. 197:887–895. doi:10.1083/jcb.201204019.

Torisawa, T., and A. Kimura. 2020. The Generation of Dynein Networks by Multi-Layered Regulation and Their Implication in Cell Division. *Front Cell Dev Biol*. 8:22. doi:10.3389/fcell.2020.00022.

Tsou, MF., T. Stearns. 2006 Mechanism limiting centrosome duplication to once per cell cycle. *Nature* 442, 947–951. doi: 10.1038/nature04985.

White, J.G., and G.G. Borisy. 1983. On the mechanisms of cytokinesis in animal cells. *J Theor Biol*. 101:289–316.

Wu, L., and A. Akhmanova. 2017. Microtubule-Organizing Centers. *Annu Rev Cell Dev Biol*. 33:51-75. Doi:10.1146/annurev-cellbio-100616-060615.

ACKNOWLEDGEMENT

I have received support from many people to advance this research. First of all, I would express my deepest appreciation to my supervisor Dr. Akatsuki Kimura for sharing with me how to advance research and how to approach science. His kindness also taught me a lot as a person. I cannot thank him enough for all his support. I would like to extend to my deep appreciation to Dr. Takayuki Torisawa for the daily discussions. His ideas and advice from a broad perspective have inspired me and helped me to grow. He also gave me a lot of mental support, which made me confident. I am extremely grateful to Ms. Tomoko Ozawa for her support in experiments and daily life. Her encouragement has made me do my best until now. I would like to express my gratitude and love to Mr. Daichi Ukai, a kind-hearted person with whom I have shared many experiences and supported each other. I am deeply indebted to Dr. Hitoshi Sawa, Dr. Yuta Shimamoto, and Dr. Yasuto Murayama for their discussions and advice on my research. With their support, I have been able to work hard on my research. I would like to extend my sincere thanks to Dr. Noritaka Masaki who taught me the basic knowledge of working with mathematics and helped me to recognize the importance of mathematics. I would like to thank Dr. Hironori Niki, Dr. Masato Kanemaki, and Dr. Hirokazu Tanimoto for their discussion and consultation on my doctoral dissertation. Many thanks to the cell architecture laboratory members, Dr. Yohei Kikuchi, Ms. Kazuko Oishi, Ms. Fumiko Iwase, Mr. Akiteru Maeno, Mr. Zenki Ikeda, Ms. Aiya Yesbolatova, Dr. Saya Ichihara, Dr. Kazunori Yamamoto, and Dr. Kenji Kimura for making my days brighter. I thank Ms. Yoko Kimura for creating the *C. elegans* strains for this study and Dr. Tomo Kondo for setting up the experimental system. I would like to thank Dr. Fumio Hanaoka, Dr.

Kazuhide Asakawa, Dr. Kei Saito, Dr. Takefumi Negishi, and Dr. Yoshiki Andachi for watching over my research life. I very much appreciate Ms. Yuki Setoguchi, Ms. Masae Inaba, Ms. Aki Sato, Ms. Hiroko Takashima, and Mr. Takeshi Shinomura for supporting my student life. A special thanks to Mr. Todd Gorman for his help with language and communication. Thanks should also go to my amazing colleagues Dr. Luwei wang, Dr. Ramasamy Kandasamy, and Dr. Takuya Hosoki. I am very grateful to have shared my time with them. Thanks also to Ms. Samal Tazhibayeva for her support every day. Finally, I would like to thank my family for accepting my choice to do a Ph.D. program and supporting me.

TABLES

Table 1: Strains used in this study

Strain	Genotype/ Description	Cultivation temperature
CAL0181	*fem-1* (*hc17ts*) *IV* (Temperature sensitive). *ruls32*[*pie-1p*::*GFP*::*H2B* + *unc-119*(+)]*III*. *ddls6* [*tbg-1*::*GFP* + *unc-119*(+)]*V*. *ltls38* [*pie-1p*::*GFP*::*PH* + *unc-119*(+)].	16°C
CAL0051	*emb-27* (*g48ts*) II (Temperature sensitive). *him-5* (*e1490*) V.	16°C
DE90	*unc-119* (*ed3* or *e2498*) *oxIs318* [*spe-11p*::*mCherry*::*histone* + *unc-119*(+)] *II*. *ruIs32* [*pie-1p*::*GFP*::*histone H2B* + *unc-119*(+)] *III*. *ddls6* [*tbg-1*::*GFP* + *unc-119*(+)]*V*. *dnls17* [*pie-1p*::*GFP*:: *PH* + *unc-119*(+)].	16 or 22°C

Table 2: Parameters for the simulations

Item	Values	References
The number of simulation steps	200	
Time per step (s)	6	
Long axis of the embryo (μm)	45.4	Experimental value
Short axes of the embryo (μm)	28.4	Experimental value
Initial coordinates of the four centrosomes (relative to the center of the embryo) (μm)	(15.7, -0.7, 1.8) (16.0, -1.8, 0.0) (-6.6, -2.7, -1.3) (-6.8, -1.8, 1.3)	Experimental values
Interval of the lattice to position the force generators (μm)	1.0	(1)
(Effective) thickness of the cortex (μm)	2.0	(1)
Pulling force by a cytoplasmic force generator (pN)	0.005	adjusted
Pulling force by an anterior cortex force generator (pN)	0.1	(1)
Pulling force by a posterior cortex force generator (pN)	0.15	(1)
Drag coefficient of the centrosome (pN s/μm)	200	(2)
The diameter of the nucleus (μm)	8	Experimental values
The stiffness of the connection between the centrosome when the nucleus is present (pN/μm)	200	adjusted

References are [1] (Kondo and Kimura, 2019), [2] (Kimura and Onami, 2010)

Supplemental Movies

Supplemental Movie S1: Centrosome movement and cell division in control *C. elegans* embryos. Time-lapse movie corresponding to Fig. 2A.

A time-lapse movie of *C. elegans* embryos expressing *GFP*::*H2B*, *tbg-1*::*GFP*, *GFP*::*PH*. In first 5 frame, the yellow arrows indicate centrosomes, yellow arrowheads indicate pronucleus and yellow circle indicates polar body. 2h imaging movies are shown in S1, S2, S3, S4 (z-maximum projections). The time indicates in minutes. The time 0 is when imaging started. Time interval is every 1min. Scale bar, 10 μm.

Supplemental Movie S2: Centrosome movement and cell division in *emb-27* (*g48ts*) mutant *C. elegans* embryos. Time-lapse movie corresponding to Fig. 2B.

Supplemental Movie S3: Centrosome movement and cell division in *klp-18* (RNAi) *C. elegans* embryos. Time-lapse movie corresponding to Fig. 2C.

Supplemental Movie S4: Centrosome movement and cell division in *emb-27* (*g48ts*) mutant and *klp-18* (RNAi) *C. elegans* embryos (enucleated embryos). Time-lapse movie corresponding to Fig. 2D.

Supplemental Movie S5: Centrosome movement in control *C. elegans* embryos during 2-cell stage. Time-lapse movie corresponding to Fig. 3B (control).

A time-lapse movie of *C. elegans* embryos expressing *GFP*::*H2B*, *tbg-1*::*GFP*, *GFP*::*PH*. In first 5 frame, the yellow arrows indicate representative sister centrosomes.

2-cell stage imaging movies are shown in S5, S6, S7 (z-maximum projections). The time indicates in minutes. The time 0 is when representative sister centrosomes were detected. Time interval is every 1min. Scale bar, 10 μm.

Supplemental Movie S6: Centrosome movement in *zyg-12* (RNAi) *C. elegans* embryos during 2-cell stage. Time-lapse movie corresponding to Fig. 3B (*zyg-12* (RNAi)).

Supplemental Movie S7: Centrosome movement in enucleated *C. elegans* embryos during 2-cell stage. Time-lapse movie corresponding to Fig. 3B and Fig. 4A (enucleated embryo).

Supplemental Movie S8: Centrosome movement in *gpr-1/2* (RNAi) in enucleated *C. elegans* embryos during 2-cell stage. Time-lapse movie corresponding to Fig. 4A (*gpr-1/2* (RNAi) enucleated embryo).

A time-lapse movie of *C. elegans* embryos expressing *GFP*::*H2B*, *tbg-1*::*GFP*, *GFP*::*PH*. In first 5 frame, the yellow arrows indicate representative sister centrosomes. 2-cell stage imaging movies are shown in S8, S9, S10, S11 (z-maximum projections). The time indicates in minutes. The time 0 is when representative sister centrosomes were detected. Time interval is every 1min. Scale bar, 10 μm.

Supplemental Movie S9: Centrosome movement in *dhc-1* (RNAi) in enucleated *C. elegans* embryos during 2-cell stage. Time-lapse movie corresponding to Fig. 4A (*dhc-1* (RNAi) enucleated embryo).

Supplemental Movie S10: Centrosome movement in *dyrb-1* (RNAi) in enucleated *C. elegans* embryos during 2-cell stage. Time-lapse movie corresponding to Fig. 4A (*dyrb-1* (RNAi) enucleated embryo).

Supplemental Movie S11: Centrosome movement in *gpr-1/2*;*dyrb-1* (RNAi) in enucleated *C. elegans* embryos during 2-cell stage. Time-lapse movie corresponding to Fig. 4A (*dyrb-1*;*gpr-1/2* (RNAi) enucleated embryo).

Supplemental Movie S12: Centrosome movement in *dhc-1* (RNAi) *C. elegans* embryos during 1-cell stage. Time-lapse movie corresponding to Fig. 6A (*dhc-1* (RNAi) embryo).

A time-lapse movie of *C. elegans* embryos expressing *GFP*::*H2B*, *tbg-1*::*GFP*, *GFP*::*PH*. In first 10 frame, the yellow arrows indicate representative sister centrosomes. 1-cell stage imaging movies are shown in S12, S13 (z-maximum projections). The time 0 is when imaging started. Time interval is every 10sec. Scale bar, 10 μm.

Supplemental Movie S13: Centrosome movement in *dhc-1*;*nmy-2* (RNAi) *C. elegans* embryos during 1-cell stage. Time-lapse movie corresponding to Fig. 6A (*nmy-2;dhc-1* (RNAi) embryo).

Supplemental Movie S14: Centrosome movement in *dhc-1* (RNAi) in enucleated *C. elegans* embryos. Time-lapse movie corresponding to Fig. 7A (*dhc-1* (RNAi)

enucleated embryo).

A time-lapse movie of *C. elegans* embryos expressing *GFP*::*H2B*, *tbg-1*::*GFP*, *GFP*::*PH*. In first 5 frame, the yellow arrows indicate centrosomes. 2h imaging movie is shown (z-maximum projections). The time 0 is when representative sister centrosomes were detected (See Fig. 4A). Time interval is every 1 min. Scale bar, 10 μm.